Performance Analysis of the Idle Mode Capability in a Dense Heterogeneous Cellular Network

Chuan Ma, Ming Ding, *Senior Member, IEEE*, David López-Pérez, *Senior Member, IEEE*, Zihuai Lin, *Senior Member, IEEE*, Jun Li, *Senior Member, IEEE*, and Guoqiang Mao, *Fellow, IEEE*

***Abstract*— In this paper, we study the impact of the base station (BS) idle mode capacity (IMC) on the network performance of multi-tier and dense heterogeneous cellular networks (HCNs) with both line-of-sight (LoS) and non-line-of-sight transmissions. Different from most existing works that investigated network scenarios with an infinite number of user equipments (UEs), we consider a more practical set-up with a finite number of UEs in our analysis. Moreover, in our model, the small BSs (SBSs) apply a positive power bias in the cell association procedure, so that macrocell UEs are actively encouraged to use the more lightly loaded SBSs. In addition, to address the severe interference that these cell range expanded UEs may suffer, the macro BSs (MBSs) apply enhanced inter-cell interference coordination, in the form of almost blank subframe (ABS) mechanism. For this model, we derive the coverage probability and the rate of a typical UE in the whole network or a certain tier. The impact of the IMC on the performance of the network is shown to be significant. In particular, it is important to note that there will be a surplus of BSs when the BS density exceeds the UE density, and thus a large number of BSs switch off. As a result, the overall coverage probability, as well as the area spectral efficiency, will continuously increase with the BS density, addressing the network outage that occurs when all BSs are active and the interference becomes LoS dominated. Finally, the optimal ABS factors are investigated in different BS density regions. One of major findings is that MBSs should give up all resources in favor of the SBSs when the small cell networks go ultra-dense. This reinforces the need for orthogonal deployments, shedding new light on the design and deployment of the future 5G dense HCNs.**

***Index Terms*— LoS and NLoS transmissions, IMC, HPPP, ultra dense network.**

Manuscript received August 15, 2017; revised January 13, 2018 and March 20, 2018; accepted March 24, 2018. Date of publication April 3, 2018; date of current version September 14, 2018. This work is supported in part by the National Natural Science Foundation of China under Grants 61727802, 61501238, and 61571128, in part by the Jiangsu Provincial Science Foundation under Project BK20150786, in part by the Specially Appointed Professor Program in Jiangsu Province, 2015, in part by the Fundamental Research Funds for the Central Universities under Grant 30916011205, and in part by the Open Research Fund of National Mobile Communications Research Laboratory, Southeast University, under Grant No. 2017D04. The associate editor coordinating the review of this paper and approving it for publication was M. Di Renzo. *(Corresponding author: Jun Li.)*

C. Ma is with the School of Electrical and Information Engineering, The University of Sydney, Sydney, NSW 2006, Australia, and also with Data61, CSIRO, Sydney, NSW 2015, Australia (e-mail: chuan.ma@sydney.edu.au).

M. Ding is with Data61, CSIRO, Sydney, NSW 2015, Australia (e-mail: ming.ding@data61.csiro.au).

D. López-Pérez is with Nokia Bell Labs, Dublin 15, Ireland (e-mail: david.lopez-perez@nokia-bell-labs.com)

Z. Lin is with the School of Electrical and Information Engineering, The University of Sydney, Sydney, NSW 2006, Australia, and also with the Fujian Provincial Engineering Technology Research Center of Photoelectric Sensing Application, Fujian Normal University, Fuzhou 350007, China (e-mail: zihuai.lin@sydney.edu.au; linzihuai@ieee.org).

J. Li is with the School of Electronic and Optical Engineering, Nanjing University of Science and Technology, Nanjing 210094, China, also with the National Mobile Communications Research Laboratory, Southeast University, Nanjing 210009, China, and also with the Department of Software Engineering, Institute of Cybernetics, National Research Tomsk Polytechnic University, 634050 Tomsk, Russia (e-mail: jun.li@njust.edu.cn).

G. Mao is with the School of Electrical and Data Engineering, University of Technology Sydney, Broadway, NSW 2007, Australia (e-mail:g.mao@ieee.org).

Color versions of one or more of the figures in this paper are available online at http://ieeexplore.ieee.org.

Digital Object Identifier 10.1109/TCOMM.2018.2822805

I. Introduction

TO MEET the explosively increasing demand for more mobile data traffic [1], commercial wireless networks are evolving towards higher frequency reuse by deploying more and more small cells [2]. A major part of the mobile throughput growth has already been supplied by the so-called *network densification* during the past few years, and this trend is expected to continue in the years to come. Thus, the emerging fifth generation (5G) cellular network deployments are envisaged to be heterogeneous and dense. Such a dense heterogeneous cellular network (HCN) will be comprised of a conventional cellular network overlaid with a variety of small cells, metro, pico and femtocells. This will greatly help to realize the 5G requirement of a 100x increase in mobile network throughput with respect to the current 4G one [3].

In this context, the co-channel deployment of macro cell BSs (MBSs) and small cell BSs (SBSs) in HCNs, i.e., all BS tiers operating on the same frequency spectrum, have recently attracted considerable attention, e.g., [4], [5] and [6]. Andrews *et al.* [7] first analyzed the coverage probability of a single-tier small cell network by modeling BS locations as a homogeneous point Poisson process (HPPP). That study concluded that the coverage probability of the network does not depend on the density of BSs in interference-limited scenarios. Following [7], Dhillon *et al.* [8] also reached the same conclusion for each BS tier in a multi-tier HCN. In contrast, using a different modelling that considered a dual slope path loss model, Zhang and Andrews [9] demonstrated that the coverage probability strongly depends on the BS density. In the same line, using a multi-slope path loss model and the smallest path loss association rule, Ding *et al.* [10] showed that the coverage probability first increases with the BS density and then decreases, while the area spectral efficiency (ASE) will grow almost linearly as the BS density goes asymptotically large. In [11], a stretched exponential path loss model was proposed for the short-range communication, and they proved

that the ASE is non-decreasing with the BS density and converges to a constant for high densities.

However, it is important to note that the aforementioned studies assumed an unlimited number of user equipment (UE) in the network, which implies that all BSs would always be active and transmit in all time and frequency resources. Obviously, this may not be the case in practice, especially in ultra-dense networks (UDNs). To attain a more practical network performance, Lee and Huang [12] first analyzed the coverage probability of a single-tier small cell network with a finite number of UEs, and derived the optimal BS density accordingly. This was done considering the tradeoff between the performance gain and the resultant network cost. Moreover, a system-level analysis of cellular networks with respect of the density of BSs and blockages was conducted in [13], which show the validity for the footprints of buildings in dense urban environments. A trackable performance analysis was proposed in [14], and they found that the increasing trend of the ASE is highly related to the density of BSs and UEs. Recently, Ding *et al.* [15] studied the coverage probability and ASE of a single-tier small cell network with probabilistic line-of-sight (LoS) and non-LoS (NLoS) transmissions, in which the UE number is finite and the small cell BS has an idle mode capability (IMC). More specifically, if there is no active UE within the coverage area of a certain BS, that BS will be turned off and will not transmit. The IMC switches off unused BSs, and thus can improve the UEs' coverage probability and network energy efficiency as the network density increases. This is because UEs can receive stronger signals from the closer BSs, while the interference power remains constant or even decreases thanks to the IMC. This conclusion in [15] - the coverage probability depends on the density of BSs in a interference-limited network - is fundamentally different from the previous results in [7] and [8], and presented new insights for the design and deployment of 5G networks.

Nevertheless, although of importance, none of the above works considered that the original association/coverage areas of the SBSs tend to be much smaller than those of the MBSs in a HCN due to the large power difference, and thus the UE population that is offloaded to small cells may be limited. To encourage UEs to take advantage of the large amount of resource at the SBSs, cell range expansion (CRE) was introduced in long term evolution (LTE) networks to proactively offload UEs from MBSs to SBSs. This is done by adding a positive offset to the pilot RSS of the SBSs during the cell selection procedure [2]. CRE allows UE not associating with the BS that providing the strongest signal strength, but with those with more resources. Intuitively speaking, more UEs will be offloaded to the SBSs with a larger range expansion bias (REB). CRE without interference management has been shown to increase the sum capacity of the macrocell UEs due to the offloading, but decrease the overall throughput of the network due to strong cell-edge interference [16]. The offloaded UEs do not connect to the strongest cell anymore. To address this cell-edge performance issue, the use of enhanced intercell interference coordination (eICIC) schemes was also introduced in LTE networks [17], [18]. One such eICIC strategy implemented in the time-domain, called almost blank subframe (ABS), received a lot of attention. No control or data signals but only reference signals are transmitted in an ABS. Thus, when a MBS schedules ABSs, SBSs can schedule their offloaded UEs in subframes overlapping with the MBS ABSs. This significantly reduces interference towards those the offloaded UEs.

To the best of our knowledge, the theoretical study of dense HCNs with a realistic path loss model, a finite number of UEs as well as CRE together with ABSs has not been conducted before, although some preliminary simulation results can be found in [2] and [19]. Motivated by this theoretical gap, in this paper, we analyze for the first time the coverage probability and ASE of a HCN with *i)* two BS tiers, *ii)* a general and practical path loss model, *iii)* a finite number of UEs, *iv)* an IMC at small cell BSs, and *v)* a flexible cell association strategy with CRE and ABS.

This results in a completely new modelling and analysis, through which we provide the following theoretical contributions:

1) We calculate an analytical expression to derive the density of active BSs in a two tier HCN. Based on this, we compute the analytical expressions of the coverage probability and ASE for such two tier HCN, while considering the IMC.
2) The optimal ABS factor, i.e., the ratio between the number of ABS to the numbers of total subframes, is showed numerically and obtained by simulations for scheduling in MBSs for different SBS density regions. Moreover, we prove that ASE can achieve the maximum value if the ABS factor is set to one when the small cell networks go ultra-dense.
3) We perform an extensive simulation campaign to validate the accuracy of the analytical results. Both simulation and analytical results match and shed new insights on the design and deployment of BSs in 5G UDNs. One important finding is that MBSs should give up all resources in favour of the SBSs when the small cell network goes ultra-dense. This reinforces the need for orthogonal spectrum assignments for macrocell and ultra-dense small cell deployments.

The rest of the paper is structured as follows. We introduce the system model in Section II, and derive the activated BS density in a two tier HCN in Section III. In Section IV, we obtain the analytical expressions of the coverage probability and ASE for this network. Then, we validate the accuracy of the analytical results through extensive simulations and discuss the network performance in Section V, and conclude the paper in Section VI.

II. System Model

In this paper, we assume a wireless network consisting of two BS tiers. The locations of the BSs of the kth tier ($k = 1, 2$) are modeled as a two-dimensional HPPP Φ_k with a density λ_k. Without loss of generality, we denote the macrocell tier and the small cell tier as tier 1 and tier 2. The locations of UEs (denoted by $\mathcal{U}$) in the network are modeled as another independent HPPP Φ_u with a density λ_u. In most existing

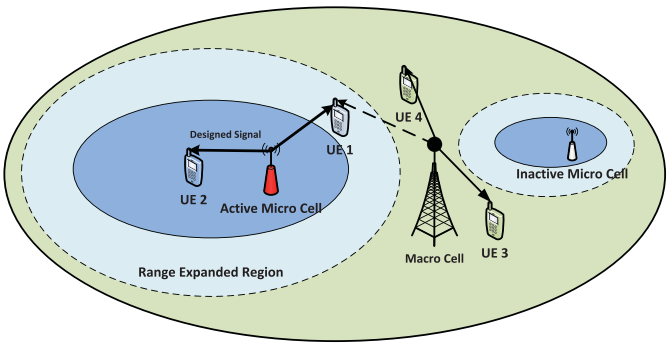

Fig. 1. A network scenario consisting of two BS tiers. Each UE is connected to the BS that provides the strongest average signal, which is marked by the designed signal. BSs with no UE associated are in idle mode.

works, λ_u was assumed to be sufficiently large, so that each BS in each tier always has at least one associated UE. However, in our model with finite BS and UE densities, a BS might serve no UE, and thus be turned off thanks to the IMC.[1]

Following [10], we adopt a general and practical path loss model, in which the path loss $\zeta(r)$ associated with distance r is calculated as

$$\zeta_k(r)=\begin{cases}\zeta_k^{\mathrm{L}}(r)=A_k^{\mathrm{L}}r^{-\alpha_k^{\mathrm{L}}}, & \text{LoS: } \mathrm{Pr}_k^{\mathrm{L}}(r);\\ \zeta_k^{\mathrm{NL}}(r)=A_k^{\mathrm{NL}}r^{-\alpha_k^{\mathrm{NL}}}, & \text{NLoS: } \mathrm{Pr}_k^{\mathrm{NL}}(r)=1-\mathrm{Pr}_k^{\mathrm{L}}(r),\end{cases} \tag{1}$$

where A_k^{L} and A_k^{NL} are the path losses at a reference distance $r=1$ for the kth tier and for the LoS and the NLoS cases, respectively, and α_k^{L} and α_k^{NL} are the path loss exponents for the kth and for the LoS and NLoS cases, respectively. Moreover, $\mathrm{Pr}_k^{\mathrm{L}}(r)$ is the LoS probability function that a transmitter and a receiver separated by a distance r has a LoS path. For example, as recommended by the 3GPP, $\mathrm{Pr}_k^{\mathrm{L}}(r)$ is can be computed as

$$\mathrm{Pr}_k^{\mathrm{L}}(r)=\begin{cases}\min\left(0.018/r,1\right)*\left(1-\exp(-r/0.063)\right)\\ +\exp(-r/0.063), & \text{when k=1;}\\ 0.5-\min(0.5,5\exp(-0.156/r))\\ +\min(0.5,5\exp(-r/0.03)), & \text{when k=2.}\end{cases} \tag{2}$$

Moreover, we consider a cell association based on the maximum received power, where a UE is associated with the strongest BS:

$$\mathcal{X}_k=P_k\zeta_k(r)D_k, \tag{3}$$

where P_k and D_k denote the transmit power and the REB of a BS in the kth tier, where $D_1=0$ dB for the macrocell tier and $D_2=D$ dB for the small cell tier.

Since UEs are randomly and uniformly distributed in the network, we adopt a common assumption that the activated BSs in each tier also follows an independent HPPP distribution $\widetilde{\Phi}_i$, the density of which is denoted by $\widetilde{\lambda_i}$ BSs/km^2 [22], [23].[2]

[1]The mobility of UEs is not considered in the work. It is worth noting that if mobility is present, MBSs may not be turned off easily, as the MBSs need to support the UE handover. Several works considering the mobility can be found in [20] and [21].

[2]Part of this work was published in IEEE WCNC 2018 [23].

Finally, we assume that each UE/BS is equipped with an isotropic antenna, and as a common practice in the field, that the multi-path fading between an arbitrary UE and an arbitrary BS is modeled as independently identical distributed (i.i.d) Rayleigh fading.

The SINR of the typical UE with a random distance r to its associated BS in the kth tier is given by

$$\mathrm{SINR}_k(r)=\frac{P_k h_{k0}\zeta_k(r)}{\sum_{j=1}^{K}\sum_{i\in\widetilde{\Phi}\setminus b_0}P_j h_{ji}\zeta_j(|Y_{ji}|)+\sigma^2}, \tag{4}$$

where h_{k0} and h_{ji} are the exponentially distributed channel power with unit mean from the serving BS and the i-th interfering BS in the j-th tier, respectively, $|Y_{ji}|$ is the distance from the activated BS in the j-th tier to the origin, and b_0 is the serving BS in the k-th tier. Note that only the activated BSs in $\widetilde{\Phi}\setminus b_0$ inject effective interference into the network, since the other BSs are turned off thanks to the IMC.

In Fig. 1, we show an illustration of the proposed network, which consists of two BS tiers. In this case, UE 1 is offloaded from the MBS to the SBS because of the REB. The other SBS is in idle mode since there is no UE associated to it.

III. Density of the Activated BSs

To evaluate the impact of the IMC on the performance of each BS tier, we first analyze the probability of having a given average number of UEs in each cell. Then, we derive expressions for the density of active BSs in each tier.

A. Average Number of UEs in Each Cell

The coverage area of each small cell is a random variable V, representing the size of a Poisson Voronoi cell. Although there is no known closed-form expression for V's probability distribution function (PDF), some accurate estimates of this distribution have been proposed in the literature, e.g., [24] and [25].

In [24], a simple gamma distribution derived from Monte Carlo simulations was used to approximate the PDF of V for the kth BS tier, given by

$$f_{V_k}(x)=(b\lambda_k)^q x^{q-1}\frac{\exp(-b\lambda_k x)}{\Gamma(q)}, \tag{5}$$

where q and b are fixed values, $\Gamma(x)=\int_0^{+\infty}t^{x-1}e^{-t}dt$ is the standard gamma function and λ_k is the BS density of the kth BS tier.

Remind here we assume the coverage area of each cell has not been considered the associating relation to users, where each user may be covered by multiple BSs in different tiers, and the average number of UEs in each cell may be a litter larger than the actual one. This inaccuracy is shown to be ignorable in the Sec. V-A. If the association probability is considered here, such that each user can only be covered by one BS, then the Poisson Voronoi cell will change to be a weighted cell, and the shape of cell will become irregular. The works in [26] show how to calculate the weighted Poisson Voronoi cell and are useful for further discussion.

Since the distribution of UEs follows a HPPP with a density of λ_u, given a Voronoi cell with size x, the number of UEs

located in this Voronoi cell is a Poisson random variable with a mean of $\lambda_u x$. Denoting by N_k the number of UEs located in a Voronoi cell of the kth BS tier, we have that

$$\mathbb{P}[N_k = n] = \int_0^{+\infty} \frac{(\lambda_u x)^n}{n!} \exp(-\lambda_u x) f_{V_k}(x) dx \overset{(a)}{=} \frac{\Gamma(n+q)}{\Gamma(n+1)\Gamma(q)} \left(\frac{\lambda_u}{\lambda_u + b\lambda_k}\right)^n \left(\frac{b\lambda_k}{\lambda_u + b\lambda_k}\right)^q, \quad n \geq 0 \quad (6)$$

where step *(a)* is computed by using the definition of the gamma function.

B. Probability of a UE Associated to the kth Tier

According to (3), each BS tier density and transmit power determine the probability that a typical UE is associated with a BS in this tier. The following Lemmas provide the per-tier association probability, which is essential for deriving the main results in the sequel.

If one UE connects to one MBS ($k = 1$), this MBS can be a MBS with an LoS path or a NLoS path. In the following, we provide the probability that one such UE is associated with an LoS MBS in Lemma 1.

Lemma 1: The probability that the UE is associated with a LoS MBS can be written as

$$\mathbb{P}_1^{\mathrm{L}} = \int_0^{\infty} p_{11}^{\mathrm{L}}(r) \times p_{12}^{\mathrm{L}}(r) \times p_{13}^{\mathrm{L}}(r) \times f_1^{\mathrm{L}}(r) dr, \quad (7)$$

where $p_{11}^{\mathrm{L}}(r) = \exp\left(-\int_0^{\Delta_{11}^{\mathrm{L}}(r)} \Pr_1^{\mathrm{NL}}(u) \times 2\pi u \lambda_1 du\right)$,
$\Delta_{11}^{\mathrm{L}}(r) = (\frac{A_1^{\mathrm{NL}}}{A_1^{\mathrm{L}}})^{\frac{1}{\alpha_1^{\mathrm{NL}}}} r^{\frac{\alpha_1^{\mathrm{L}}}{\alpha_1^{\mathrm{NL}}}}$, *and*
$p_{12}^{\mathrm{L}}(r) = \exp\left(-\int_0^{\Delta_{12}^{\mathrm{L}}(r)} \Pr_2^{\mathrm{L}}(u) \times 2\pi u \lambda_2 du\right)$,
$\Delta_{12}^{\mathrm{L}}(r) = \left(\frac{DP_2 A_2^{\mathrm{L}}}{P_1 A_1^{\mathrm{L}}}\right)^{\frac{1}{\alpha_2^{\mathrm{L}}}} r^{\frac{\alpha_1^{\mathrm{L}}}{\alpha_2^{\mathrm{L}}}}$, *and*
$p_{13}^{\mathrm{L}}(r) = \exp\left(-\int_0^{\Delta_{13}^{\mathrm{L}}(r)} \Pr_2^{\mathrm{NL}}(u) \times 2\pi u \lambda_2 du\right)$,
$\Delta_{13}^{\mathrm{L}}(r) = \left(\frac{DP_2 A_2^{\mathrm{NL}}}{P_1 A_1^{\mathrm{L}}}\right)^{\frac{1}{\alpha_2^{\mathrm{NL}}}} r^{\frac{\alpha_1^{\mathrm{L}}}{\alpha_2^{\mathrm{NL}}}}$, *respectively, and* $f_1^{\mathrm{L}}(r)$ *is the PDF of that the UE is associated with a LoS MBS, which can be written as*

$$f_1^{\mathrm{L}}(r) = \exp\left\{-\int_0^r \Pr_1^{\mathrm{L}}(u) 2\pi\lambda_1 u du\right\} \times \Pr_1^{\mathrm{L}}(r) 2\pi\lambda_1 r. \quad (8)$$

Proof: See Appendix A. ∎

Following the same logic, we provide the probability that the UE is associated with a NLoS MBS in Lemma 2.

Lemma 2: The probability that the UE is associated with a NLoS MBS can be written as

$$\mathbb{P}_1^{\mathrm{NL}} = \int_0^{\infty} p_{11}^{\mathrm{NL}}(r) \times p_{12}^{\mathrm{NL}}(r) \times p_{13}^{\mathrm{NL}}(r) \times f_1^{\mathrm{NL}}(r) dr, \quad (9)$$

where $p_{11}^{\mathrm{NL}}(r) = \exp\left(-\int_0^{\Delta_{11}^{\mathrm{NL}}(r)} \Pr_1^{\mathrm{L}}(u) \times 2\pi u \lambda_1 du\right)$,
$\Delta_{11}^{\mathrm{NL}}(r) = (\frac{A_1^{\mathrm{L}}}{A_1^{\mathrm{NL}}})^{\frac{1}{\alpha_1^{\mathrm{L}}}} \times r^{\frac{\alpha_1^{\mathrm{NL}}}{\alpha_1^{\mathrm{L}}}}$, *and*
$p_{12}^{\mathrm{NL}}(r) = \exp\left(-\int_0^{\Delta_{12}^{\mathrm{NL}}(r)} \Pr_2^{\mathrm{L}}(u) \times 2\pi u \lambda_2 du\right)$,
$\Delta_{12}^{\mathrm{NL}}(r) = \left(\frac{DP_2 A_2^{\mathrm{L}}}{P_1 A_1^{\mathrm{NL}}}\right)^{\frac{1}{\alpha_2^{\mathrm{L}}}} \times r^{\frac{\alpha_1^{\mathrm{NL}}}{\alpha_2^{\mathrm{L}}}}$, *and*
$p_{13}^{\mathrm{NL}}(r) = \exp\left(-\int_0^{\Delta_{13}^{\mathrm{NL}}(r)} \Pr_2^{\mathrm{NL}}(u) \times 2\pi u \lambda_2 du\right)$,
$\Delta_{13}^{\mathrm{NL}}(r) = \left(\frac{DP_2 A_2^{\mathrm{NL}}}{P_1 A_1^{\mathrm{NL}}}\right)^{\frac{1}{\alpha_2^{\mathrm{NL}}}} \times r^{\frac{\alpha_1^{\mathrm{NL}}}{\alpha_2^{\mathrm{NL}}}}$, *respectively, and* $f_1^{\mathrm{NL}}(r)$ *is the PDF that the UE is associated with a NLoS MBS, which can be written as*

$$f_1^{\mathrm{NL}}(r) = \exp\left\{-\int_0^r \Pr_1^{\mathrm{NL}}(u) 2\pi\lambda_1 u du\right\} \times \Pr_1^{\mathrm{NL}}(r) 2\pi\lambda_1 r. \quad (10)$$

Proof: See Appendix B. ∎

If one UE connects to one SBS ($K = 2$), this SBS can also be a SBS with an LoS path or a NLoS path. Similarly, the corresponding UE association probabilities are derived in Lemma 3 and Lemma 4.

Lemma 3: The probability that the UE is associated with a LoS SBS can be written as

$$\mathbb{P}_2^{\mathrm{L}} = \int_0^{\infty} p_{21}^{\mathrm{L}}(r) \times p_{22}^{\mathrm{L}}(r) \times p_{23}^{\mathrm{L}}(r) \times f_2^{\mathrm{L}}(r) dr, \quad (11)$$

where $p_{21}^{\mathrm{L}}(r) = \exp(-\int_0^{\Delta_{21}^{\mathrm{L}}} \Pr_1^{\mathrm{NL}}(u) \times 2\pi u \lambda_1 du)$,
$\Delta_{21}^{\mathrm{L}}(r) = (\frac{P_1 A_1^{\mathrm{L}}}{DP_2 A_2^{\mathrm{L}}})^{\frac{1}{\alpha_1^{\mathrm{L}}}} \times r^{\frac{\alpha_2^{\mathrm{L}}}{\alpha_1^{\mathrm{L}}}}$, *and*
$p_{22}^{\mathrm{L}}(r) = \exp(-\int_0^{\Delta_{22}^{\mathrm{L}}} \times \Pr_1^{\mathrm{L}}(u) 2\pi u \lambda_1 du)$,
$\Delta_{22}^{\mathrm{L}}(r) = (\frac{P_1 A_1^{\mathrm{NL}}}{DP_2 A_2^{\mathrm{L}}})^{\frac{1}{\alpha_1^{\mathrm{NL}}}} r^{\frac{\alpha_2^{\mathrm{L}}}{\alpha_1^{\mathrm{NL}}}}$, *and*
$p_{23}^{\mathrm{L}}(r) = \exp(-\int_0^{\Delta_{23}^{\mathrm{L}}} \Pr_2^{\mathrm{NL}}(u) \times 2\pi u \lambda_2 du)$,
$\Delta_{23}^{\mathrm{L}}(r) = (\frac{A_2^{\mathrm{NL}}}{A_2^{\mathrm{L}}})^{\frac{1}{\alpha_2^{\mathrm{NL}}}} \times r^{\frac{\alpha_2^{\mathrm{L}}}{\alpha_2^{\mathrm{NL}}}}$, *respectively, and*
$f_2^{\mathrm{L}}(r) = \Pr_2^{\mathrm{L}}(r) 2\pi\lambda_2 r \times \exp\left\{-\int_0^r \Pr_2^{\mathrm{L}}(u) 2\pi\lambda_2 u du\right\}$.

Lemma 4: The probability that the UE is associated with a NLoS SBS can be written as

$$\mathbb{P}_2^{\mathrm{NL}} = \int_0^{\infty} p_{21}^{\mathrm{NL}}(r) \times p_{22}^{\mathrm{NL}}(r) \times p_{23}^{\mathrm{NL}}(r) \times f_2^{\mathrm{NL}}(r) dr, \quad (12)$$

where $p_{21}^{\mathrm{NL}}(r) = \exp(-\int_0^{\Delta_{21}^{\mathrm{NL}}} \times \Pr_1^{\mathrm{L}}(u) 2\pi u \lambda_1 du)$,
$\Delta_{21}^{\mathrm{NL}}(r) = (\frac{P_1 A_1^{\mathrm{L}}}{DP_2 A_2^{\mathrm{NL}}})^{\frac{1}{\alpha_1^{\mathrm{L}}}} \times r^{\frac{\alpha_2^{\mathrm{NL}}}{\alpha_1^{\mathrm{L}}}}$, *and*
$p_{22}^{\mathrm{NL}}(r) = \exp(-\int_0^{\Delta_{22}^{\mathrm{NL}}} \times \Pr_1^{\mathrm{NL}}(u) 2\pi u \lambda_1 du)$,
$\Delta_{22}^{\mathrm{NL}}(r) = (\frac{P_1 A_1^{\mathrm{NL}}}{DP_2 A_2^{\mathrm{NL}}})^{\frac{1}{\alpha_1^{\mathrm{NL}}}} \times r^{\frac{\alpha_2^{\mathrm{NL}}}{\alpha_1^{\mathrm{NL}}}}$, *and*
$p_{23}^{\mathrm{NL}}(r) = \exp(-\int_0^{\Delta_{23}^{\mathrm{NL}}} \Pr_2^{\mathrm{L}}(u) \times 2\pi u \lambda_2 du)$,
$\Delta_{23}^{\mathrm{NL}}(r) = (\frac{A_2^{\mathrm{L}}}{A_2^{\mathrm{NL}}})^{\frac{1}{\alpha_2^{\mathrm{L}}}} \times r^{\frac{\alpha_2^{\mathrm{NL}}}{\alpha_2^{\mathrm{L}}}}$, *respectively, and*
$f_2^{\mathrm{NL}}(r) = \exp\left\{-\int_0^r \Pr_2^{\mathrm{NL}}(u) 2\pi\lambda_2 u du\right\} \times \Pr_2^{\mathrm{NL}}(r) 2\pi\lambda_2 r$.

Proof: The proofs of Lemma 3 and Lemma 4 are similar with Lemma 1 and Lemma 2, so the proof are omitted here. ∎

C. Density of Activated BSs in the kth Tier

After attaining the probability of one UE associating to a BS in the kth tier, we are ready to derive the density of active BSs in the kth tier.

Defining by $\mathbb{P}_k^{\mathrm{off}}(n)$ the probability that a BS in the kth tier is inactive when there are n UEs in its coverage, then $\mathbb{P}_k^{\mathrm{off}}(n)$ can be calculated by

$$\mathbb{P}_k^{\mathrm{off}}(n) = \mathbb{P}[N_k = n](1 - A_k)^n, \quad (13)$$

where $\mathbb{P}[N_k = n]$ is the probability of having n UEs located in a cell of the kth tier, which can be obtained from (6), and $A_k = \mathbb{P}_k^{\mathrm{L}} + \mathbb{P}_k^{\mathrm{NL}}$, which denotes the per-tier association probability.

With this result, the density of active BSs in the kth tier $\widetilde{\lambda}_k$ can now be derived as

$$\widetilde{\lambda}_k = \lambda_k \left(1 - \sum_{n=0}^{\infty} \mathbb{P}_k^{\mathrm{off}}(n)\right), \tag{14}$$

where $\mathbb{P}_k^{\mathrm{off}}(n)$ is the probability that the kth tier is inactive when there are n UEs in its coverage.

IV. Main Results

Recall that in this paper, The REB for the first tier (macro tier) is $D_1 = 0\ dB$ and that for the second tier is simply denoted by D, where $D \geq 0\ dB$.

With our modelling, a UE $u \in \mathcal{U}$ belongs to the following six disjoint sets:

$$u \in \begin{cases} \mathcal{U}_1 \begin{cases} \mathcal{U}_1^{\mathrm{L}}, & \text{The UE connects to a LoS MBS;} \\ \mathcal{U}_1^{\mathrm{NL}}; & \text{The UE connects to a NLoS MBS;} \end{cases} \\ \mathcal{U}_2 \begin{cases} \mathcal{U}_2^{\mathrm{L}}, & \text{The UE connects to a LoS SBS without power bias;} \\ \mathcal{U}_2^{\mathrm{NL}}; & \text{The UE connects to a NLoS SBS without power bias;} \end{cases} \\ \mathcal{U}_3 \begin{cases} \mathcal{U}_3^{\mathrm{L}}, & \text{The UE is offloaded from a MBS to a LoS SBS;} \\ \mathcal{U}_3^{\mathrm{NL}}; & \text{The UE is offloaded from a MBS to a NLoS SBS,} \end{cases} \end{cases} \tag{15}$$

where $\mathcal{U}_1 \bigcup \mathcal{U}_2 \bigcup \mathcal{U}_3 = \mathcal{U}$. The set $\mathcal{U}_1$ is the set of macrocell UEs and the set $\mathcal{U}_2$ is the set of unbiased small cell UEs. The UEs offloaded from macrocells to small cells due to CRE constitute set $\mathcal{U}_3$, and are referred to as *range expanded (RE) UEs.*

Moreover, an ABS approach to eICIC is considered, in which MBSs shut their transmissions on certain fraction of time/frequency resources, and SBSs schedule their RE UEs on the corresponding resources, which are free from macrocell interference.

Definition 1: η: The resource partitioning fraction η is the fraction of resources on which the MBSs are inactive, where $0 < \eta < 1$. η is also known as the ABS factor.

Thus, with resource partitioning, $1 - \eta$ is the fraction of resources that the MBSs and the SBSs allocate to UEs in $\mathcal{U}_1$ and $\mathcal{U}_2$, respectively, while η is the fraction of resources in which the MBSs do not transmit and the SBSs can schedule UEs in $\mathcal{U}_2$ and $\mathcal{U}_3$.

In Fig. 2, we show an illustration of the proposed network when the ABS framework is in place. When the MBS schedules ABSs and mutes its transmission, UE 3 and UE 4 will not receive any signal from their serving MBS. In contrast, the UEs associated with the SBS, i.e., UE 1 (the RE SBS UE) and UE 2 (the native SBS UE), can be served without the interference from the MBS.

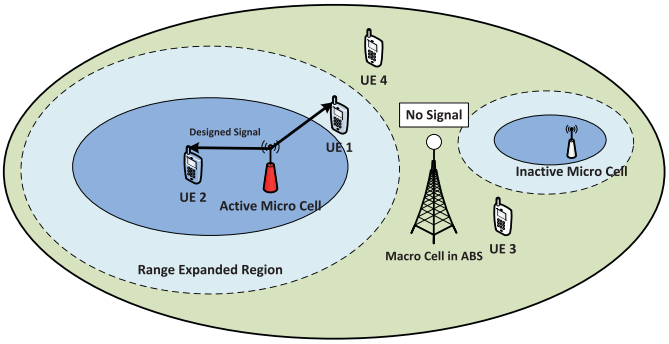

Fig. 2. MBS schedules ABSs, and the UEs associated with it cannot get service in such subframes.

As a result of resource partitioning, the SINR of a typical UE u, when it belongs to $\mathcal{U}_k$, can be written as

$$\mathrm{SINR} = \mathbf{1}(k \in 1,2)\frac{P_k h_{k,0}\zeta_k(r)}{\sum_{k=1}^{2} I_k + \sigma^2} + \mathbf{1}(k \in 2,3)\frac{P_2 h_{2,0}\zeta_2(r)}{I_2 + \sigma^2}, \tag{16}$$

where $\mathbf{1}(A)$ is the indicator of the event A, and I_k is the interference from the kth tier.

A. The Coverage Probability

Let us define the coverage probability $\mathcal{S}$ as the probability that the instantaneous SINR of a randomly located UE is larger than a target SINR (τ). Since the typical UE is associated with at most one BS, the coverage probability can be calculated by

$$\mathcal{S} = \sum_{k=1}^{3} \mathcal{S}_k = \sum_{k=1}^{3} \mathbb{P}(\mathrm{SINR}_k > \tau). \tag{17}$$

The results of the coverage probability is presented in Theorem 1 shown on the top of next page.

In Theorem 1, $\mathcal{L}_I(s)$ in (20), as shown at the top of the next page, are the Laplace transform of I_{agg} evaluated at s for LoS or NLoS transmissions in each BS tier, respectively. For clarity, they are presented in the following Lemmas.

Lemma 5: In Theorem 1, $\mathcal{L}_{I_1^{\mathrm{L/NL}}}(s)$ are given by

$$\mathcal{L}_{I_1^{\mathrm{L}}}(s) = \exp\left(-2\pi\tilde{\lambda}_1 \int_x^{\infty} \mathrm{Pr}_1^{\mathrm{L}}(u)\frac{u}{1 + \frac{S_1^{\mathrm{L}}(x)}{\tau S_1^{\mathrm{L}}(u)}}du\right) \times \exp\left(-2\pi\tilde{\lambda}_1 \int_{\Delta_{11}^{\mathrm{L}}(x)}^{\infty} \mathrm{Pr}_1^{\mathrm{NL}}(u)\frac{u}{1 + \frac{S_1^{L}(x)}{\tau S_1^{\mathrm{NL}}(u)}}du\right) \times \exp\left(-2\pi\tilde{\lambda}_2 \int_{\Delta_{12}^{\mathrm{L}}(x)}^{\infty} \mathrm{Pr}_2^{\mathrm{L}}(u)\frac{u}{1 + \frac{S_1^{\mathrm{L}}(x)}{\tau S_2^{\mathrm{L}}(u)}}du\right) \times \exp\left(-2\pi\tilde{\lambda}_2 \int_{\Delta_{13}^{\mathrm{L}}(x)}^{\infty} \mathrm{Pr}_2^{\mathrm{NL}}(u)\frac{u}{1 + \frac{S_1^{\mathrm{L}}(x)}{\tau S_2^{\mathrm{NL}}(u)}}du\right), \tag{21}$$

Theorem 1 (Coverage Probability): For a typical UE in the presented framework, the SINR *coverage probability is*

$$\mathcal{S}(\tau)=\mathcal{S}_1^{\mathrm{L}}(\tau)+\mathcal{S}_1^{\mathrm{NL}}(\tau)+\mathcal{S}_2^{\mathrm{L}}(\tau)+\mathcal{S}_2^{\mathrm{NL}}(\tau)+\mathcal{S}_3^{\mathrm{L}}(\tau)+\mathcal{S}_3^{\mathrm{NL}}(\tau), \tag{18}$$

where $\mathcal{S}_1^{\mathrm{L/NL}}(\tau) = \int_0^\infty \Pr\left[\frac{S_1^{\mathrm{L/NL}}(x)h}{I_{\mathrm{agg}}+\sigma^2}>\tau\right]\mathcal{F}_1^{\mathrm{L/NL}}(x)dx$, $S_2^{\mathrm{L/NL}}(\tau) = \theta\int_0^\infty \Pr\left[\frac{S_2^{\mathrm{L/NL}}(x)h}{I_{\mathrm{agg}_1}+\sigma^2}>\tau\right]\mathcal{F}_2^{\mathrm{L/NL}}(x)dx + (1-\theta)\int_0^\infty \Pr\left[\frac{S_2^{\mathrm{L/NL}}(x)h}{I_{\mathrm{agg}_2}+\sigma^2}>\tau\right]\mathcal{F}_2^{\mathrm{L/NL}}(x)dx$, *and* $\mathcal{S}_3^{\mathrm{L/NL}}(\tau)=\int_0^\infty \Pr\left[\frac{S_3^{\mathrm{L/NL}}(x)h}{I_{\mathrm{agg}}+\sigma^2}>\tau\right]\mathcal{F}_3^{\mathrm{L/NL}}(x)dx$, *where* θ *represents the ABS fraction, and* $\theta=1-\eta$. *Moreover,* $\mathcal{F}_1^{\mathrm{L/NL}}(x)dx$, $\mathcal{F}_2^{\mathrm{L/NL}}(x)dx$ *and* $\mathcal{F}_3^{\mathrm{L/NL}}(x)dx$ *are represented by*

$$\begin{aligned}
\mathcal{F}_1^{\mathrm{L/NL}}(x) &= p_{11}^{\mathrm{L/NL}}(x)\times p_{12}^{\mathrm{L/NL}}(x)\times p_{13}^{\mathrm{L/NL}}(x)\times f_1^{\mathrm{L/NL}}(x),\\
\mathcal{F}_2^{\mathrm{L/NL}}(x) &= p_{21}^{\mathrm{L'/NL'}}(x)\times p_{22}^{\mathrm{L'/NL'}}(x)\times p_{23}^{\mathrm{L/NL}}(x)\times f_2^{\mathrm{L/NL}}(x),\\
\mathcal{F}_3^{\mathrm{L}}(x) &= p_{21}^{\mathrm{L}}(x)\times p_{22}^{\mathrm{L}}(x)\times p_{23}^{\mathrm{L}}(x)\times\left(\mathfrak{p}_1^{\mathrm{L}}(x)+\mathfrak{p}_1^{\mathrm{NL}}(x)\right)\times f_2^{\mathrm{L}}(x),\ \textit{and}\\
\mathcal{F}_3^{\mathrm{NL}}(x) &= p_{21}^{\mathrm{NL}}(x)\times p_{22}^{\mathrm{NL}}(x)\times p_{23}^{\mathrm{NL}}(x)\times\left(\mathfrak{p}_2^{\mathrm{L}}(x)+\mathfrak{p}_2^{\mathrm{NL}}(x)\right)\times f_2^{\mathrm{NL}}(x).
\end{aligned} \tag{19}$$

In addition, $\Pr\left[\frac{S_1^{\mathrm{L/NL}}(x)h}{I_{\mathrm{agg}}+\sigma^2}>\tau\right]$, $\Pr\left[\frac{S_2^{\mathrm{L/NL}}(x)h}{I_{\mathrm{agg}_{1,2}}+\sigma^2}>\tau\right]$ *and* $\Pr\left[\frac{S_3^{\mathrm{L/NL}}(x)h}{I_{\mathrm{agg}}+\sigma^2}>\tau\right]$ *are respectively computed by*

$$\begin{aligned}
\Pr\left[\frac{S_1^{\mathrm{L/NL}}(x)h}{I_{\mathrm{agg}}+\sigma^2}>\tau\right] &= \exp\left(-\frac{\sigma^2\tau}{S_1^{\mathrm{L/NL}}(x)}\right)\times\mathcal{L}_{I_1^{\mathrm{L/NL}}}\left(\frac{\tau}{S_1^{\mathrm{L/NL}}(x)}\right),\\
\Pr\left[\frac{S_2^{\mathrm{L/NL}}(x)h}{I_{\mathrm{agg}_1}+\sigma^2}>\tau\right] &= \exp\left(-\frac{\sigma^2\tau}{S_2^{\mathrm{L/NL}}(x)}\right)\times\mathcal{L}_{I_{21}^{\mathrm{L/NL}}}\left(\frac{\tau}{S_2^{\mathrm{L/NL}}(x)}\right),\\
\Pr\left[\frac{S_2^{\mathrm{L/NL}}(x)h}{I_{\mathrm{agg}_2}+\sigma^2}>\tau\right] &= \exp\left(-\frac{\sigma^2\tau}{S_2^{\mathrm{L/NL}}(x)}\right)\times\mathcal{L}_{I_{22}^{\mathrm{L/NL}}}\left(\frac{\tau}{S_2^{\mathrm{L/NL}}(x)}\right),\textit{and}\\
\Pr\left[\frac{S_3^{\mathrm{L/NL}}(x)h}{I_{\mathrm{agg}}+\sigma^2}>\tau\right] &= \exp\left(-\frac{\sigma^2\tau}{S_2^{\mathrm{L/NL}}(x)}\right)\times\mathcal{L}_{I_3^{\mathrm{L/NL}}}\left(\frac{\tau}{S_2^{\mathrm{L/NL}}(x)}\right).
\end{aligned} \tag{20}$$

Proof: See Appendix C. ∎

and

$$\begin{aligned}
\mathcal{L}_{I_1^{\mathrm{NL}}}(s) = &\exp\left(-2\pi\tilde{\lambda}_1\int_x^\infty \Pr_1^{\mathrm{NL}}(u)\frac{u}{1+\frac{S_1^{\mathrm{NL}}(x)}{\tau S_1^{\mathrm{NL}}(u)}}du\right)\\
&\times\exp\left(-2\pi\tilde{\lambda}_1\int_{\Delta_{11}^{\mathrm{NL}}(x)}^\infty \Pr_1^{\mathrm{L}}(u)\frac{u}{1+\frac{S_1^{\mathrm{NL}}(x)}{\tau S_1^{\mathrm{L}}(u)}}du\right)\\
&\times\exp\left(-2\pi\tilde{\lambda}_2\int_{\Delta_{12}^{\mathrm{NL}}(x)}^\infty \Pr_2^{\mathrm{L}}(u)\frac{u}{1+\frac{S_1^{\mathrm{NL}}(x)}{\tau S_2^{\mathrm{L}}(u)}}du\right)\\
&\times\exp\left(-2\pi\tilde{\lambda}_2\int_{\Delta_{13}^{\mathrm{NL}}(x)}^\infty \Pr_2^{\mathrm{NL}}(u)\frac{u}{1+\frac{S_1^{\mathrm{NL}}(x)}{\tau S_2^{\mathrm{NL}}(u)}}du\right).
\end{aligned} \tag{22}$$

In Lemma 5, the interference from a LoS/NLoS channel for a UE $u\in\mathcal{U}_1$ is represented by (21) and (22), respectively. Moreover, the interference for $\mathcal{L}_{I_1^L}$ is composed of four parts, which are from other LoS MBSs, NLoS MBSs, LoS SBSs and NLoS SBSs as showed in (21), and $\mathcal{L}_{I_1^{NL}}$ is shown as the similar components.

Lemma 6: In Theorem 1, $\mathcal{L}_{I_{21}^{\mathrm{L/NL}}}(s)$ *and* $\mathcal{L}_{I_{22}^{\mathrm{L/NL}}}(s)$ *are given by*

$$\begin{aligned}
\mathcal{L}_{I_{21}^{\mathrm{L}}}(s) = &\exp\left(-2\pi\tilde{\lambda}_1\int_{\Delta_{21}^{\mathrm{L'}}(x)}^\infty \Pr_1^{\mathrm{L}}(u)\frac{u}{1+\frac{S_2^{\mathrm{L}}(x)}{\tau S_1^{\mathrm{L}}(u)}}du\right)\\
&\times\exp\left(-2\pi\tilde{\lambda}_1\int_{\Delta_{22}^{\mathrm{L'}}(x)}^\infty \Pr_1^{\mathrm{NL}}(u)\frac{u}{1+\frac{S_2^{\mathrm{L}}(x)}{\tau S_1^{\mathrm{NL}}(u)}}du\right)\\
&\times\exp\left(-2\pi\tilde{\lambda}_2\int_x^\infty \Pr_2^{\mathrm{L}}(u)\frac{u}{1+\frac{S_2^{\mathrm{L}}(x)}{\tau S_2^{\mathrm{L}}(u)}}du\right)\\
&\times\exp\left(-2\pi\tilde{\lambda}_2\int_{\Delta_{23}^{\mathrm{L}}(x)}^\infty \Pr_2^{\mathrm{NL}}(u)\frac{u}{1+\frac{S_2^{\mathrm{L}}(x)}{\tau S_2^{\mathrm{NL}}(u)}}du\right).
\end{aligned} \tag{23}$$

$$\begin{aligned}
\mathcal{L}_{I_{22}^{\mathrm{L}}}(s) = &\exp\left(-2\pi\tilde{\lambda}_2\int_x^\infty \Pr_2^{\mathrm{L}}(u)\frac{u}{1+\frac{S_2^{\mathrm{L}}(x)}{\tau S_2^{\mathrm{L}}(u)}}du\right)\\
&\times\exp\left(-2\pi\tilde{\lambda}_2\int_{\Delta_{23}^{\mathrm{L}}(x)}^\infty \Pr_2^{\mathrm{NL}}(u)\frac{u}{1+\frac{S_2^{\mathrm{L}}(x)}{\tau S_2^{\mathrm{NL}}(u)}}du\right);
\end{aligned} \tag{24}$$

and

$$\begin{aligned}
\mathcal{L}_{I_{21}^{\mathrm{NL}}}(s) = &\exp\left(-2\pi\tilde{\lambda}_1\int_{\Delta_{21}^{\mathrm{NL}'}(x)}^\infty \Pr_1^{\mathrm{L}}(u)\frac{u}{1+\frac{S_2^{\mathrm{NL}}(x)}{\tau S_1^{\mathrm{L}}(u)}}du\right)\\
&\times\exp\left(-2\pi\tilde{\lambda}_1\int_{\Delta_{22}^{\mathrm{NL}'}(x)}^\infty \Pr_1^{\mathrm{NL}}(u)\frac{u}{1+\frac{S_2^{\mathrm{NL}}(x)}{\tau S_1^{\mathrm{NL}}(u)}}du\right)\\
&\times\exp\left(-2\pi\tilde{\lambda}_2\int_{\Delta_{23}^{\mathrm{NL}}(x)}^\infty \Pr_2^{\mathrm{L}}(u)\frac{u}{1+\frac{S_2^{\mathrm{NL}}(x)}{\tau S_2^{\mathrm{L}}(u)}}du\right)\\
&\times\exp\left(-2\pi\tilde{\lambda}_2\int_x^\infty \Pr_2^{\mathrm{NL}}(u)\frac{u}{1+\frac{S_2^{\mathrm{NL}}(x)}{\tau S_2^{\mathrm{NL}}(u)}}du\right),
\end{aligned} \tag{25}$$

$$\mathcal{L}_{I_{22}^{\mathrm{NL}}}(s) = \exp\left(-2\pi\tilde{\lambda}_2 \int_{\Delta_{23}^{\mathrm{NL}}(x)}^{\infty} \mathrm{Pr}_2^{\mathrm{L}}(u) \frac{u}{1+\frac{S_2^{\mathrm{NL}}(x)}{\tau S_1^{\mathrm{L}}(u)}} du\right) \times \exp\left(-2\pi\tilde{\lambda}_2 \int_{x}^{\infty} \mathrm{Pr}_2^{\mathrm{NL}}(u) \frac{u}{1+\frac{S_2^{\mathrm{NL}}(x)}{\tau S_2^{\mathrm{NL}}(u)}} du\right). \tag{26}$$

In Lemma 6, the interference from a LoS/NLoS channel for a UE $u \in \mathcal{U}_2$ is represented in (23)-(26), respectively. Moreover, from (24) we can find that when the ABS is working, only the interference from the other SBSs is valid. This is because all the MBSs are not transmitting in the ABS, and this brings about two parts of interference in (24). Similar components are shown in (25) and (26).

Lemma 7: In Theorem 1, $\mathcal{L}_{I_3^{\mathrm{L/NL}}}(s)$ are given by

$$\mathcal{L}_{I_3^{\mathrm{L}}}(s) = \exp\left(-2\pi\tilde{\lambda}_2 \int_{x}^{\infty} \mathrm{Pr}_2^{\mathrm{L}}(u) \frac{u}{1+\frac{S_2^{\mathrm{L}}(x)}{\tau S_2^{\mathrm{L}}(u)}} du\right) \times \exp\left(-2\pi\tilde{\lambda}_2 \int_{\Delta_{23}^{\mathrm{L}}(x)}^{\infty} \mathrm{Pr}_2^{\mathrm{NL}}(u) \frac{u}{1+\frac{S_2^{\mathrm{L}}(x)}{\tau S_2^{\mathrm{NL}}(u)}} du\right), \tag{27}$$

and

$$\mathcal{L}_{I_3^{\mathrm{NL}}}(s) = \exp\left(-2\pi\tilde{\lambda}_2 \int_{\Delta_{23}^{\mathrm{NL}}(x)}^{\infty} \mathrm{Pr}_2^{\mathrm{L}}(u) \frac{u}{1+\frac{S_2^{\mathrm{NL}}(x)}{\tau S_2^{\mathrm{L}}(u)}} du\right) \times \exp\left(-2\pi\tilde{\lambda}_2 \int_{x}^{\infty} \mathrm{Pr}_2^{\mathrm{NL}}(u) \frac{u}{1+\frac{S_2^{\mathrm{NL}}(x)}{\tau S_2^{\mathrm{NL}}(u)}} du\right). \tag{28}$$

In Lemma 7, the interference from a LoS/NLoS channel for a UE $u \in \mathcal{U}_3$ is represented in (27) and (28), respectively. Similar with (24) and (26), the components of them are two pars, as the interference only comes from SBSs.

It is important to note that the impact of the tier and BS selection on the coverage probability is measured in (19), the expressions of which are based on λ_1 and λ_2. This is because all the BSs can be chosen by the UEs. Moreover, the impact of the interference on the coverage probability is measured in Lemma 5, 6 and 7. Note that instead of λ_1 and λ_2, we use $\tilde{\lambda}_1$ and $\tilde{\lambda}_2$. This is because we use the IMC, and thus only the activated BSs emit effective interference into the network.

B. Area Spectral Efficiency

In this subsection, we investigate the network capacity performance in terms of the area spectral efficiency (ASE) in bps/HZ/km^2, which is defined as

$$R = \sum_{k\in 1,2,3} \mathbf{1}(u \in \mathcal{U}_k)\eta_k \mathcal{R}_k, \tag{29}$$

where $\mathbf{1}(A)$ is the indicator of the event A, $\eta_1 = 1-\eta$, $\eta_3 = \eta$, and $\eta_2 = 1-\eta$ when ABS is engaged, while $\eta_2 = \eta$ when ABS is not engaged.

Then, the per tier $\mathcal{R}_k$ is defined by

$$\mathcal{R}_k \triangleq \lambda_u \mathbb{E}_x\left\{\mathbb{E}_{\mathrm{SINR}_k}[\log_2(1+\mathrm{SINR}_k(x))]\right\}. \tag{30}$$

It is important to note that the average is taken over both the spatial PPP and the channel fading distribution. The ASE is first averaged on the condition that the typical UE is at a distance x from its serving BS in the kth tier. Then it is averaged by calculating the expectation over the distance x. The following Theorem 2 on the top of next page gives the ASE over the entire network.

Although the results for the coverage probability and ASE are not in closed-form, they can be numerically evaluated in a simple form. Moreover, they can be presented in closed-form expressions in several cases, for example, the 3GPP Case 1 mentioned in [10].

C. Special Case for ASE

In this subsection, we use a special case to show the analysis results for the ASE, and obtain insights from it.

We consider a very dense network that $\lambda_2 \to +\infty$, then the signal comes from the NLoS BSs can be neglected, and all UEs can be assumed to connect with BSs in a LoS channel. Thus, the ASE for the considered very dense network does not actually depend on the LoS and NLoS propagation, and it can be described as the following Lemma.

Lemma 8: In a very dense network that $\lambda_2 \to +\infty$, the ASE can be shown as

$$\begin{aligned} R &= \mathcal{R}_1^{\mathrm{L}} + \mathcal{R}_2^{\mathrm{L}} + \mathcal{R}_3^{\mathrm{L}} \\ &= (1-\eta)\lambda_u(\Theta_1 + \Theta_{21}) + \eta\lambda_u(\Theta_{22} + \Theta_3), \end{aligned} \tag{38}$$

where

$$\Theta_1 = \int_{x=0}^{\infty}\int_{\rho_0}^{\infty} \exp\left(-\frac{\sigma^2 t(\rho)}{S_1^{\mathrm{L}}(x)}\right) \times \mathcal{L}_{I_1^{\mathrm{L}}}\left(\frac{t(\rho)}{S_1^{\mathrm{L}}(x)}\right) d\rho \mathcal{F}_1^{\mathrm{L}}(x) dx, \tag{39}$$

$$\Theta_{21} = \int_{x=0}^{\infty}\int_{\rho_0}^{\infty} \exp\left(-\frac{\sigma^2 t(\rho)}{S_2^{\mathrm{L}}(x)}\right) \times \mathcal{L}_{I_{21}^{\mathrm{L}}}\left(\frac{t(\rho)}{S_2^{\mathrm{L}}(x)}\right) d\rho \mathcal{F}_2^{\mathrm{L}}(x) dx, \tag{40}$$

$$\Theta_{22} = \int_{x=0}^{\infty}\int_{\rho_0}^{\infty} \exp\left(-\frac{\sigma^2 t(\rho)}{S_2^{\mathrm{L}}(x)}\right) \times \mathcal{L}_{I_{22}^{\mathrm{L}}}\left(\frac{t(\rho)}{S_2^{\mathrm{L}}(x)}\right) d\rho \mathcal{F}_2^{\mathrm{L}}(x) dx, \tag{41}$$

and

$$\Theta_3 = \int_{x=0}^{\infty}\int_{\rho_0}^{\infty} \exp\left(-\frac{\sigma^2 t(\rho)}{S_2^{\mathrm{L}}(x)}\right) \times \mathcal{L}_{I_3^{\mathrm{L}}}\left(\frac{t(\rho)}{S_2^{\mathrm{L}}(x)}\right) d\rho \mathcal{F}_3^{\mathrm{L}}(x) dx. \tag{42}$$

Besides, to compute the interference power for different tiers, $\mathcal{L}_{I_1^{L}}(\frac{t(\rho)}{S_1^{L}(x)})$,$\mathcal{L}_{I_{21}^{L}}(\frac{t(\rho)}{S_2^{L}(x)})$, $\mathcal{L}_{I_{22}^{L}}(\frac{t(\rho)}{S_2^{L}(x)})$, and $\mathcal{L}_{I_3^{L}}(\frac{t(\rho)}{S_2^{L}(x)})$, we propose Lemma 9.

Lemma 9: The interference power for different tiers can be calculated by

$$\mathcal{L}_{I_1^{\mathrm{L}}}\left(\frac{t(\rho)}{S_1^{\mathrm{L}}(x)}\right) = \exp\left(-2\pi\widetilde{\lambda_1} \times \rho\left(\alpha_1^L, 1, t(\rho)^{-1} x^{-\alpha_1^L}, x\right)\right)$$

Theorem 2 (Area Spectral Efficiency): For a typical user in the setup, the ASE *is computed by*

$$R = \mathcal{R}_1^{\mathrm{L}} + \mathcal{R}_1^{\mathrm{NL}} + \mathcal{R}_2^{\mathrm{L}} + \mathcal{R}_2^{\mathrm{NL}} + \mathcal{R}_3^{\mathrm{L}} + \mathcal{R}_3^{\mathrm{NL}}, \tag{31}$$

where the conditional rate coverage $\mathcal{R}_k$ is given by the following equations:

$$\mathcal{R}_1^{\mathrm{L}} = (1-\eta)\lambda_u \int_{x=0}^{\infty}\int_{\rho_0}^{\infty} \exp\left(-\frac{\sigma^2 t(\rho)}{S_1^{\mathrm{L}}(x)}\right) \times \mathcal{L}_{I_1^{\mathrm{L}}}\left(\frac{t(\rho)}{S_1^{\mathrm{L}}(x)}\right) d\rho \mathcal{F}_1^{\mathrm{L}}(x)dx; \tag{32}$$

$$\mathcal{R}_1^{\mathrm{NL}} = (1-\eta)\lambda_u \int_{x=0}^{\infty}\int_{\rho_0}^{\infty} \exp\left(-\frac{\sigma^2 t(\rho)}{S_2^{\mathrm{L}}(x)}\right) \times \mathcal{L}_{I_1^{\mathrm{NL}}}\left(\frac{t(\rho)}{S_1^{\mathrm{NL}}(x)}\right) d\rho \mathcal{F}_2^{\mathrm{L}}(x)dx; \tag{33}$$

$$\begin{aligned}\mathcal{R}_2^{\mathrm{L}} &= (1-\eta)\lambda_u \int_{x=0}^{\infty}\int_{\rho_0}^{\infty} \exp\left(-\frac{\sigma^2 t(\rho)}{S_2^{\mathrm{L}}(x)}\right) \times \mathcal{L}_{I_{21}^{\mathrm{L}}}\left(\frac{t(\rho)}{S_2^{\mathrm{L}}(x)}\right) d\rho \mathcal{F}_2^{\mathrm{L}}(x)dx \\ &\quad + \eta\lambda_u \int_{x=0}^{\infty}\int_{\rho_0}^{\infty} \exp\left(-\frac{\sigma^2 t(\rho)}{S_2^{\mathrm{L}}(x)}\right) \times \mathcal{L}_{I_{22}^{\mathrm{L}}}\left(\frac{t(\rho)}{S_2^{\mathrm{L}}(x)}\right) d\rho \mathcal{F}_2^{\mathrm{L}}(x)dx;\end{aligned} \tag{34}$$

$$\begin{aligned}\mathcal{R}_2^{\mathrm{NL}} &= (1-\eta)\lambda_u \int_{x=0}^{\infty}\int_{\rho_0}^{\infty} \exp\left(-\frac{\sigma^2 t(\rho)}{S_2^{\mathrm{NL}}(x)}\right) \times \mathcal{L}_{I_{21}^{\mathrm{NL}}}\left(\frac{t(\rho)}{S_2^{\mathrm{NL}}(x)}\right) d\rho \mathcal{F}_2^{\mathrm{NL}}(x)dx; \\ &\quad + \eta\lambda_u \int_{x=0}^{\infty}\int_{\rho_0}^{\infty} \exp\left(-\frac{\sigma^2 t(\rho)}{S_2^{\mathrm{NL}}(x)}\right) \times \mathcal{L}_{I_{22}^{\mathrm{NL}}}\left(\frac{t(\rho)}{S_2^{\mathrm{NL}}(x)}\right) d\rho \mathcal{F}_2^{\mathrm{NL}}(x)dx\end{aligned} \tag{35}$$

$$\mathcal{R}_3^{\mathrm{L}} = \eta\lambda_u \int_{x=0}^{\infty}\int_{\rho_0}^{\infty} \exp\left(-\frac{\sigma^2 t(\rho)}{S_2^{\mathrm{L}}(x)}\right) \times \mathcal{L}_{I_3^{\mathrm{L}}}\left(\frac{t(\rho)}{S_2^{\mathrm{L}}(x)}\right) d\rho \mathcal{F}_3^{\mathrm{L}}(x)dx; \tag{36}$$

$$\mathcal{R}_3^{\mathrm{NL}} = \eta\lambda_u \int_{x=0}^{\infty}\int_{\rho_0}^{\infty} \exp\left(-\frac{\sigma^2 t(\rho)}{S_2^{\mathrm{NL}}(x)}\right) \times \mathcal{L}_{I_3^{\mathrm{NL}}}\left(\frac{t(\rho)}{S_2^{\mathrm{NL}}(x)}\right) d\rho \mathcal{F}_3^{\mathrm{NL}}(x)dx, \tag{37}$$

where $\rho_0 = \log_2(\tau+1)$, defined the minimum working SINR*, and $t(\rho) = 2^{\rho}-1$ and the* PDFs *in each equation are given in Theorem 2.*

Proof: See Appendix D. ∎

$$\times \exp\left(-2\pi\widetilde{\lambda_2}\times\rho\left(\alpha_2^L, 1, \frac{P_1 A_1^L}{P_2 A_2^L} t(\rho)^{-1} x^{-\alpha_1^L}, \Delta_{12}^{L,}(x)\right)\right), \tag{43}$$

$$\begin{aligned}&\mathcal{L}_{I_{21}^{\mathrm{L}}}\left(\frac{t(\rho)}{S_2^{\mathrm{L}}(x)}\right) \\ &= \exp\left(-2\pi\widetilde{\lambda_1}\times\rho\left(\alpha_1^L, 1, \frac{P_2 A_2^L}{P_1 A_1^L} t(\rho)^{-1} x^{-\alpha_2^L}, \Delta_{21}^{L,\prime}(x)\right)\right) \\ &\quad \times \exp\left(-2\pi\widetilde{\lambda_2}\times\rho\left(\alpha_2^L, 1, t(\rho)^{-1} x^{-\alpha_2^L}, x\right)\right),\end{aligned} \tag{44}$$

and

$$\begin{aligned}\mathcal{L}_{I_{22}^{\mathrm{L}}}\left(\frac{t(\rho)}{S_2^{\mathrm{L}}(x)}\right) &= \mathcal{L}_{I_3^{\mathrm{L}}}\left(\frac{t(\rho)}{S_2^{\mathrm{L}}(x)}\right) \\ &= \exp\left(-2\pi\widetilde{\lambda_2}\times\rho\left(\alpha_2^L, 1, t(\rho)^{-1} x^{-\alpha_2^L}, x\right)\right),\end{aligned} \tag{45}$$

where

$$\begin{aligned}&\rho(\alpha,\beta,t,d) \\ &= \left[\frac{d^{-(\alpha-\beta-1)}}{t(\alpha-\beta-1)}\right] {}_2F_1\left[1, 1-\frac{\beta+1}{\alpha}; 2-\frac{\beta+1}{\alpha}; -\frac{1}{td^{\alpha}}\right], \\ &\qquad (\alpha > \beta+1),\end{aligned} \tag{46}$$

where ${}_2F_1[\cdot,\cdot;\cdot;\cdot]$ is the hyper-geometric function [27].

Proof: See Appendix E. ∎

From Lemma 8 and 9, the expression of the special case can be obtained, where the expressions of the interference power are much simpler than in the general case. To get more insights, we provide Lemma 10 to show that the ASE achieves the maximum value when the ABS factor is set to one.

Lemma 10: In a very dense network, ASE achieves the maximum value when the ABS factor is set to one.

Proof: Take the derivative of R with respect to η, then we get $\frac{\Delta R}{\Delta \eta} = \Theta_{22} + \Theta_3 - \Theta_1 - \Theta_{21}$. As the $\lambda_2 \to +\infty$, for the UE associated with a MBS, the interference power is increasing while the source power keeps stable. For the UE associated with a SBS, the UE can get stronger signal from a closer SBS. So intuitively speaking, $\Theta_{22} + \Theta_3$, which represents the UE connecting the SBS and receiving interference only from SBSs, should larger than $\Theta_1 + \Theta_{21}$, which suffers interferences from all BSs. As a result, $\frac{\Delta R}{\Delta \eta} > 0$ and the optimal ABS factor should be one to get the maximum ASE. ∎

V. Simulation and Discussion

In this section, we use numerical results to establish the accuracy of our analysis, and further study the performance of dense HCNs.

A. Validation and Discussion on the Active BS Probability

We consider the 2-tier HCN, following the 3GPP definitions [28], to show the accuracy of our analysis. Table I summarizes the most important assumptions and parameter values.

In Fig. 3, we plot $\mathbb{P}_i^{\mathrm{on}}$ versus λ_2, where $\lambda_2 \in [10, 1000]$ BSs/km^2. As can be observed from this figure, our analytical results match well with the simulation results. Moreover, they also show that, within the 5 dB power bias allocation to the small cell BSs, *i)* the probability of a BS being active in the

TABLE I
PARAMETER VALUES SUMMARY

Parameter	Values
Macro BS transmit power P_1	46 dBm
Micro BS transmit power P_2	24 dBm
Macro BS density λ_1	10 BSs/km^2
User density λ_u	300 UEs/km2
A_1^{L}	$10^{-10.34}$
α_1^{L}	2.42
A_1^{NL}	$10^{-13.11}$
α_1^{NL}	4.28
A_2^{L}	$10^{-10.38}$
α_2^{L}	2.09
A_2^{NL}	$10^{-14.54}$
α_2^{NL}	3.75
Power bias allocation D	5 dB
Noise Power σ^2	-95 dBm
$q = b$	4.18 [15]
Resource partitioning fraction η	0.4

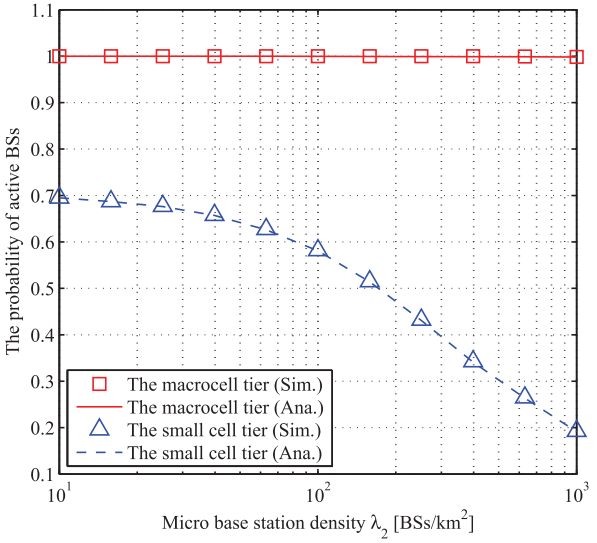

Fig. 3. The active BS probability for each tier.

small cell BS tier decreases with λ_2, when λ_u is a finite value, and that *ii)* the BSs with a lower transmit power have lower activation probability. For example, more than 60% of the BSs in the small cell BS tier are idle when $\lambda_2 > 300$ BSs/km^2. This means that a large number of UEs are associated with the BSs in the macrocell tier, as they can provide stronger signals to these UEs.

B. Validation and Discussion on the Coverage Probability

In this subsection, we first validate the accuracy of Theorem 1. As in the previous subsection, the network consists of 2 tiers of BSs, representing as $\mathcal{U}_1$ and $\mathcal{U}_2$, respectively, and $\mathcal{U}_3$ is defined by the small cell tier, contributed by the range expanded (RE) UEs. All the simulation results are represented by the solid line.

In Fig. 4, we show the results of $\mathcal{S}$ with respect to λ_2. As can be seen from the figure, there are some small misalignment between the simulation and analytical results in each tier. For example, there is about 1.5% inaccuracy when λ_2 is about 16 BSs/km^2 as shown in Fig. 4. With the increasing number

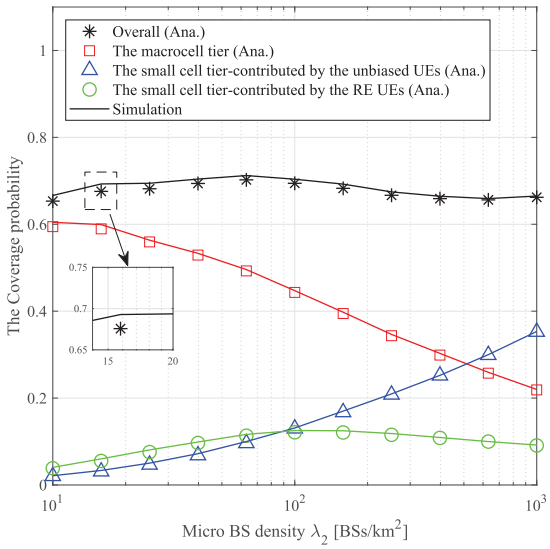

Fig. 4. The coverage probability with respect to small cell BS density λ_2.

of BSs in the small cell tier, the error becomes negligible. The reason of such error is that the spatial correlation in the UE association process is not considered in our analysis. More specially, when performing simulations, nearby UEs have a high probability of being covered and served by the same BS. However, for tractability, we consider the BS association of different UEs as independent process in (13) in our analysis, which underestimates the active BS density, as their no channel correlation. Since the accuracy of $\mathcal{S}$ is good enough, about 1.5%, we will only use analytical results of $\mathcal{S}$ for the figures in the sequel.

Fig. 4 also shows that with the increasing number of BSs in the small cell tier, the coverage probability of $\mathcal{U}_1$ decreases while that of $\mathcal{U}_2$ increases. The coverage probability of $\mathcal{U}_3$ first increases to a peak point and then decreases afterwards. As a result, the overall coverage probability first increases, then decreases, and finally increases again. The reason behind this phenomenon is that:

- The overall coverage probability first increases because UEs can connect to the stronger BSs.
- Then, the overall coverage probability decreases since the interference power grows faster than the signal power as many interfering paths transit from NLoS to LoS.
- Finally, the overall coverage probability performance continuously increases as the network densifies. The intuition is that the interference power will remain constant when the BS density is large enough (larger than the UE density), thanks to the IMC,[3] while the signal power will continuously grow due to the closer proximity of the serving BSs, as well as the larger pool of BSs to select from.

[3]The interference power will become constant eventually when there is large number of BSs. This is because of the IMC, which makes the number of active BSs at most equal to the number of UEs. Thus, from the viewpoint of the typical UE, the interference from other active BSs can be regarded as the aggregate interference generated by BSs on a HPPP plane with the same intensity as the UE intensity. Such aggregate interference is bounded and statistically stable [7].

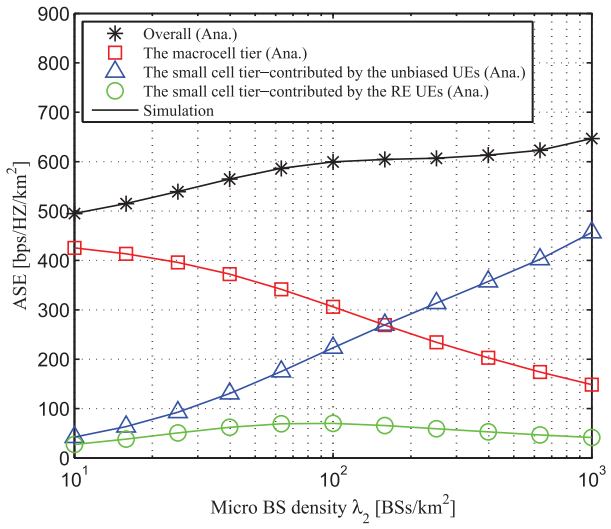

Fig. 5. The results of ASE with respect to the small cell BS density λ_2.

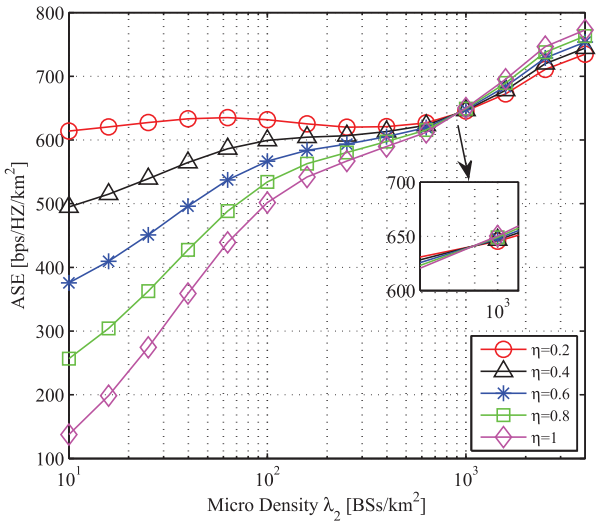

Fig. 6. The system throughput with respect to the SBS density λ_2.

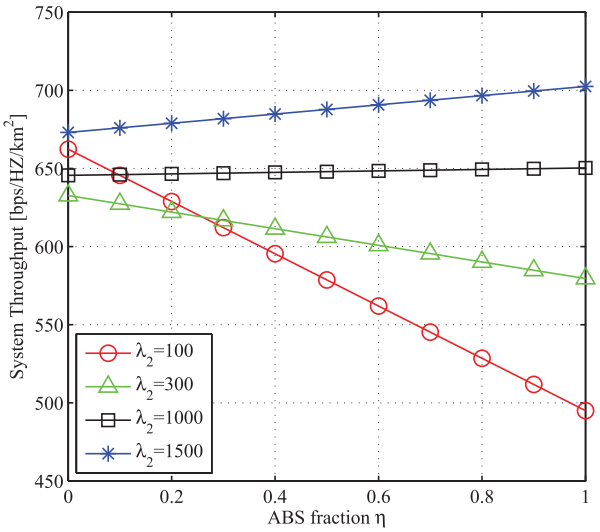

Fig. 7. The system throughput with respect to the ABS factor η.

C. Validation and Discussion on the ASE

In this subsection, we first validate the accuracy of Theorem 2, and then discuss the optimal ABS factor in different BS density regions.

In Fig. 5, we can observe that the analytical results on the per tier ASE match well with the simulation results. Moreover, the results show that with an increasing number of BSs in the small cell tier, the ASE of $\mathcal{U}_1$ decreases, while ASE of $\mathcal{U}_2$ increases. The ASE performance decrease of $\mathcal{U}_1$ is because the interference power grows, as the BSs in the small cell tier get closer and transition to LoS, while the signal power remains constant. There is no densification in the macrocell tier. The ASE performance increase of $\mathcal{U}_2$ is because the signal power grows, as the UE is served by a stronger link in the small cell tier, while the interference power remains constant. This because the BS density is larger than the UE density and due to the IMC in the small cell tier. In contrast, the offloaded UE in $\mathcal{U}_3$ will first benefit from the network densification, but later they get a more severe interference from the increasing number of BSs in the small cell tier, whereas they do not have a large serving BS pool to select from.

In Fig. 6, the ASE is showed as a function of the BS density in the small cell tier for four different ABS fractions η. Note that $\lambda_u = 300$ UEs/km^2. We can draw the following conclusions from Fig. 6:

- The ASE almost monotonically grows as the network densifies. In more detail, the system throughput first increases quickly when λ_2 goes from 10 BSs/km^2 to 100 BSs/km^2. Then, the ASE suffers from a slow growth or even a decrease when $\lambda_2 \in [100, 900]$ BSs/km^2.
  Finally, the ASE monotonically grows again when $\lambda_2 >$ 900 BSs/km^2.
- Different ABS factors should be applied in different BS density regions. In the region of $\lambda_2 < 900$ BSs/km^2, most users are associated with the MBSs and the less the number of ABSs, i.e., smaller η, the larger the ASE. However, when $\lambda_2 \geq 900$ BSs/km^2, the more the number of ABSs, i.e., lager η, the larger the ASE, since there are more users associated with the SBSs. The demarcation point, 900 BSs/km^2, should be strongly related to the REB, which in this case is 5 dB.

In Fig. 7, we verify the observations from Fig. 6 by comparing the system throughput as a function of the ABS fraction for four different BS densities in the small cell tier λ_2. Note that $\lambda_u = 300$ UEs/km^2. Four SBS densities are considered in this figure to show the various trends of the ABS fraction. As can be found from the figure, more channel resource should be allocated to the BSs in the macrocell tier when the network is sparse, e.g., $\lambda_2 = 100$ BSs/km^2 and $\lambda_2 = 300$ BSs/km^2. When the network is denser, although the service to the macrocell UEs will get affected, for the benefit of the whole system, a larger η should be applied. It is important to note that MBSs should give up all resources, all subframes are ABSs, when the small cell networks go ultra-dense. The intuition is that most

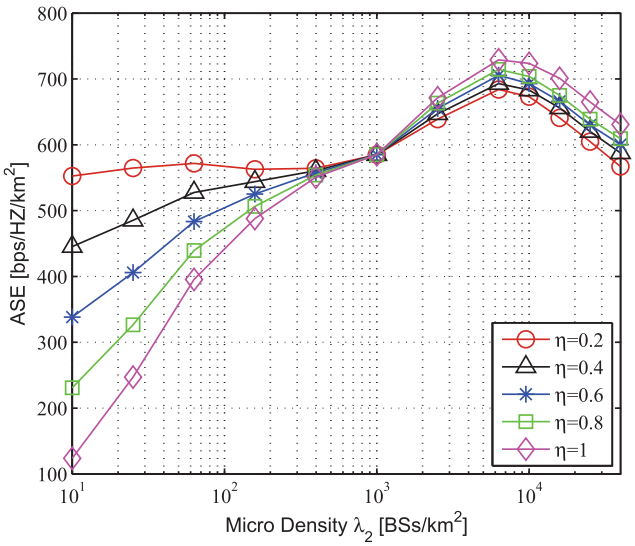

Fig. 8. The system throughput with respect to the SBS density λ_2.

UEs are associated with small cell BSs at close proximity in UDNs, and the density of small cell BSs is very large. As a result, the cost of activating a MBS is high, since it will severely interfere with a large number of small cell BSs. Therefore, using a higher η, i.e., macrocell BSs giving up more subframe resources, is helpful to achieve a better overall system throughput. This reveals an important conclusion: to maximize network capacity, ultra-dense small cell networks should operate in a different frequency spectrum from the macrocell ones. In other words, the orthogonal deployment is superior to the co-channel deployment for ultra-dense small cell networks in future wireless networks. The intuition is that the additional spatial reuse of spectrum in the co-channel deployment is over-shadowed by the large interference emitted from the macrocell tier to the ultra-dense small cell tier.

In Fig. 8, we compare the current results with the bounded path loss model in [29] as follows,

$$\zeta_k'(r) = \begin{cases} \zeta_k^{\mathrm{L}'}(r) = A_k^{\mathrm{L}}(1+r)^{-\alpha_k^{\mathrm{L}}}, \\ \text{LoS: } \Pr_k^{\mathrm{L}}(r); \\ \zeta_k^{\mathrm{NL}'}(r) = A_k^{\mathrm{NL}}(1+r)^{-\alpha_k^{\mathrm{NL}}}, \\ \text{NLoS: } \Pr_k^{\mathrm{NL}}(r) = 1 - \Pr_k^{\mathrm{L}}(r). \end{cases} \tag{47}$$

From Fig. 8 we can find that there are two main differences with previous results. The first one is the crossing point, which is about 1000 BSs/km^2, is a little bigger than that in Fig. 6. This is because of the application of the bounded path loss model, which makes the receive power smaller than the previous one, especially for the SBS UEs. Thus, more resources should be allocated in the MBSs when the density of small cell BSs is not very large, and the crossing point shifts right. The second difference is that the ASE will first increase and then decrease with the density of the SBS, and should finally keep constant [30]. The intuition is that the received signal from BSs is bounded while the interference power keeps increasing, so the ASE will decay for the denser BSs. When the network goes into ultra-dense, because of the limited number of UEs and the IMC of the BSs, the user signal power and the interference power are both bounded, so the ASE will keep constant at end. Similarly, the same conclusion can be found from the results of the ASE performance: MBSs should give up all resources when the small cell networks go ultra-dense.

VI. Conclusion

In this paper, we have studied the impact of the IMC, caused by the finite number of UEs, on the network performance in a dense two-tier HCN with LoS and NLoS transmissions. Moreover, to address the under-utilization of SBSs, CRE and eICIC via ABSs are adopted in this work. Our results show that as the BS density in the second tier surpasses the UE density, for the considered path loss model, the coverage probability and the ASE will continuously increase in this dense two-tier HCN, addressing the issue caused by the NLoS to LoS transition of interfering paths. Moreover, it is important to note that more ABSs are needed to enhance the performance of range expanded UEs as the small cell BS density grows, indicating that ultra-dense small cells should operate in a different frequency spectrum from the macrocell ones. This conclusion enlightens the new design and deployment of dense HCNs in 5G and beyond.

Appendix A
Proof of Lemma 1

In this proof we first derive the conditions that the UE is associated with a LoS MBS, which the LoS MBS provides stronger power than other BSs.

- UE is associated with a LoS MBS with no NLoS MBS inside:

$$\begin{aligned} p_{11}^{\mathrm{L}}(r) &= \Pr\left(P_1 \times A_1^{\mathrm{L}} r^{-\alpha_1^{\mathrm{L}}} > P_1 \times A_1^{\mathrm{NL}} r_1^{-\alpha_1^{\mathrm{NL}}}\right) \\ &= \Pr\left(r_1 > \left(\frac{A_1^{\mathrm{NL}}}{A_1^{\mathrm{L}}}\right)^{\frac{1}{\alpha_1^{\mathrm{NL}}}} \times r^{\frac{\alpha_1^{\mathrm{L}}}{\alpha_1^{\mathrm{NL}}}}\right) \\ &\overset{(a)}{=} \Pr(\text{No NLoS MBS closer than } \Delta_{11}^{\mathrm{L}}) \\ &= \exp\left(-\int_0^{\Delta_{11}^{\mathrm{L}}(r)} (1 - \Pr_1^{\mathrm{L}}(u)) \times 2\pi u \lambda_1 du\right), \end{aligned} \tag{48}$$

  where step (a) is given by $\Delta_{11}^{\mathrm{L}}(r) = (\frac{A_1^{\mathrm{NL}}}{A_1^{\mathrm{L}}})^{\frac{1}{\alpha_1^{\mathrm{NL}}}} \times r^{\frac{\alpha_1^{\mathrm{L}}}{\alpha_1^{\mathrm{NL}}}}$.
- UE is associated with a LoS MBS with no LoS SBS inside:

$$\begin{aligned} p_{12}^{\mathrm{L}}(r) &= \Pr\left(P_1 \times A_1^{\mathrm{L}} r^{-\alpha_1^{\mathrm{L}}} > P_2 \times A_2^{\mathrm{L}} r_2^{-\alpha_2^{\mathrm{L}}} \times D\right) \\ &= \Pr\left(r_2 > \left(\frac{A_2^{\mathrm{L}}}{A_1^{\mathrm{L}}}\right)^{\frac{1}{\alpha_2^{\mathrm{L}}}} \times D^{\frac{1}{\alpha_2^{\mathrm{L}}}} \times \left(\frac{P_2}{P_1}\right)^{\frac{1}{\alpha_2^{\mathrm{L}}}} \times r^{\frac{\alpha_1^{\mathrm{L}}}{\alpha_2^{\mathrm{L}}}}\right) \\ &\overset{(b)}{=} \Pr(\text{No LoS SBS closer than } \Delta_{12}^{\mathrm{L}}) \\ &= \exp\left(-\int_0^{\Delta_{12}^{\mathrm{L}}(r)} \Pr_2^{\mathrm{L}}(u) \times 2\pi u \lambda_2 du\right), \end{aligned} \tag{49}$$

  where step (b) is given by $\Delta_{12}^{\mathrm{L}}(r) = \left(\frac{A_2^{\mathrm{L}}}{A_1^{\mathrm{L}}}\right)^{\frac{1}{\alpha_2^{\mathrm{L}}}} \times D^{\frac{1}{\alpha_2^{\mathrm{L}}}} \times \left(\frac{P_2}{P_1}\right)^{\frac{1}{\alpha_2^{\mathrm{L}}}} \times r^{\frac{\alpha_1^{\mathrm{L}}}{\alpha_2^{\mathrm{L}}}}$.

- UE is associated with a LoS MBS with no NLoS SBS inside:

$$\begin{aligned} p_{13}^{\mathrm{L}}(r) &= \Pr\left(P_1 \times A_1^{\mathrm{L}} r^{-\alpha_1^{\mathrm{L}}} > P_2 \times A_2^{\mathrm{NL}} r_2^{-\alpha_2^{\mathrm{NL}}} \times D\right) \\ &= \Pr\left(r_2 > \left(\frac{A_2^{\mathrm{NL}}}{A_1^{\mathrm{L}}}\right)^{\frac{1}{\alpha_2^{\mathrm{NL}}}} \times D^{\frac{1}{\alpha_2^{\mathrm{NL}}}} \times \left(\frac{P_2}{P_1}\right)^{\frac{1}{\alpha_2^{\mathrm{NL}}}} \times r^{\frac{\alpha_1^{\mathrm{L}}}{\alpha_2^{\mathrm{NL}}}}\right) \\ &\overset{(c)}{=} \Pr(\text{No NLoS SBS closer than } \Delta_{13}^{\mathrm{L}}) \\ &= \exp\left(-\int_0^{\Delta_{13}^{\mathrm{L}}(r)} \left(1-\Pr_2^{\mathrm{L}}(u)\right) \times 2\pi u \lambda_2 du\right), \end{aligned} \tag{50}$$

where step (c) is given by $\Delta_{13}^{\mathrm{L}}(r) = \left(\frac{A_2^{\mathrm{NL}}}{A_1^{\mathrm{L}}}\right)^{\frac{1}{\alpha_2^{\mathrm{NL}}}} \times D^{\frac{1}{\alpha_2^{\mathrm{NL}}}} \times \left(\frac{P_2}{P_1}\right)^{\frac{1}{\alpha_2^{\mathrm{NL}}}} \times r^{\frac{\alpha_1^{\mathrm{L}}}{\alpha_2^{\mathrm{NL}}}}$.

According to [7], the CCDF of r (the distance that the nearest BS with a LoS path to the UE) is written as $\bar{F}_R^{\mathrm{L}}(r) = \exp(-\int_0^r \Pr^{\mathrm{L}}(u) 2\pi u \lambda du)$. Taking the derivative of $(1-\bar{F}_R^{\mathrm{L}}(r))$ with regard to r, we can get the PDF of r as:

$$f_1^{\mathrm{L}}(r) = \exp\left\{-\int_0^r \Pr_1^{\mathrm{L}}(u) 2\pi\lambda_1 u du\right\} \times \Pr_1^{\mathrm{L}}(r) 2\pi\lambda_1 r. \tag{51}$$

So the probability that the UE is associated with a LoS MBS can be written as

$$\mathbb{P}_1^{\mathrm{L}} = \int_0^\infty p_{11}^{\mathrm{L}}(r) \times p_{12}^{\mathrm{L}}(r) \times p_{13}^{\mathrm{L}}(r) \times f_1^{\mathrm{L}}(r) dr. \tag{52}$$

Appendix B
Proof of Lemma 2

Following the same logic with Lemma 1, the conditions that the UE is associated with a MBS with the NLoS path can be derived as:

- UE is associated with a NLoS MBS with no LoS MBS inside:

$$p_{11}^{\mathrm{NL}}(r) = \exp\left(-\int_0^{\Delta_{11}^{\mathrm{NL}}(r)} \Pr_1^{\mathrm{L}}(u) \times 2\pi u \lambda_1 du\right), \tag{53}$$

where $\Delta_{11}^{\mathrm{NL}}(r) = (\frac{A_1^{\mathrm{L}}}{A_1^{\mathrm{NL}}})^{\frac{1}{\alpha_1^{\mathrm{L}}}} \times r^{\frac{\alpha_1^{\mathrm{NL}}}{\alpha_1^{\mathrm{L}}}}$.

- UE is associated with a NLoS MBS with no LoS SBS inside:

$$p_{12}^{\mathrm{NL}}(r) = \exp\left(-\int_0^{\Delta_{12}^{\mathrm{NL}}(r)} \Pr_2^{\mathrm{L}}(u) \times 2\pi u \lambda_2 du\right), \tag{54}$$

where $\Delta_{12}^{\mathrm{NL}}(r) = \left(\frac{A_2^{\mathrm{L}}}{A_1^{\mathrm{NL}}}\right)^{\frac{1}{\alpha_2^{\mathrm{L}}}} \times D^{\frac{1}{\alpha_2^{\mathrm{L}}}} \times \left(\frac{P_2}{P_1}\right)^{\frac{1}{\alpha_2^{\mathrm{L}}}} \times r^{\frac{\alpha_1^{\mathrm{NL}}}{\alpha_2^{\mathrm{L}}}}$.

- UE is associated with a NLoS MBS with no NLoS SBS inside:

$$p_{13}^{\mathrm{NL}}(r) = \exp\left(-\int_0^{\Delta_{13}^{\mathrm{NL}}(r)} \left(1-\Pr_2^{\mathrm{NL}}(u)\right) \times 2\pi u \lambda_2 du\right), \tag{55}$$

where $\Delta_{13}^{\mathrm{NL}}(r) = \left(\frac{A_2^{\mathrm{NL}}}{A_1^{\mathrm{NL}}}\right)^{\frac{1}{\alpha_2^{\mathrm{NL}}}} \times D^{\frac{1}{\alpha_2^{\mathrm{NL}}}} \times \left(\frac{P_2}{P_1}\right)^{\frac{1}{\alpha_2^{\mathrm{NL}}}} \times r^{\frac{\alpha_1^{\mathrm{NL}}}{\alpha_2^{\mathrm{NL}}}}$.

So the probability that the UE is associated with a NLoS MBS can be written as

$$\mathbb{P}_1^{\mathrm{NL}} = \int_0^\infty p_{11}^{\mathrm{NL}}(r) \times p_{12}^{\mathrm{NL}}(r) \times p_{13}^{\mathrm{NL}}(r) \times f_1^{\mathrm{NL}}(r) dr, \tag{56}$$

where $f_1^{\mathrm{NL}}(r)$ is the PDF that the UE is associated with the NLoS MBS and can be written as

$$\begin{aligned} f_1^{\mathrm{NL}}(r) = \exp\left\{-\int_0^r \left(1-\Pr_1^{\mathrm{L}}(u)\right) 2\pi\lambda_1 u du\right\} \\ \times \left(1-\Pr_1^{\mathrm{L}}(r)\right) 2\pi\lambda_1 r. \end{aligned} \tag{57}$$

Appendix C
Proof of Theorem 1

In this proof we first analyze the case that $u \in \{\mathcal{U}_1, \mathcal{U}_2\}$, where the derivation process follows the same approach. We first derive the distribution of the distance between the typical user u and the tagged BS. Let X_l denote this distance, then

$$\mathbb{P}(X_l > x) = \mathbb{P}(X_l > x | u \in \mathcal{U}_l) = \frac{\Pr(X_l > x | u \in \mathcal{U}_l)}{\Pr(u \in \mathcal{U}_l)}. \tag{58}$$

Based on Sec. II-B and [22], the corresponding PDFs are

$$\begin{aligned} \mathcal{F}_1^{\mathrm{L}}(x) &= p_{11}^{\mathrm{L}}(x) \times p_{12}^{\mathrm{L}}(x) \times p_{13}^{\mathrm{L}}(x) \times f_1^{\mathrm{L}}(x); \\ \mathcal{F}_1^{\mathrm{NL}}(x) &= p_{11}^{\mathrm{NL}}(x) \times p_{12}^{\mathrm{NL}}(x) \times p_{13}^{\mathrm{NL}}(x) \times f_1^{\mathrm{NL}}(x); \\ \mathcal{F}_2^{\mathrm{L}}(x) &= p_{21}^{\mathrm{L'}}(x) \times p_{22}^{\mathrm{L'}}(x) \times p_{23}^{\mathrm{L}}(x) \times f_2^{\mathrm{L}}(x); \\ \mathcal{F}_2^{\mathrm{NL}}(x) &= p_{21}^{\mathrm{NL'}}(x) \times p_{22}^{\mathrm{NL'}}(x) \times p_{23}^{\mathrm{NL}}(x) \times f_2^{\mathrm{NL}}(x), \end{aligned} \tag{59}$$

where

$$\begin{cases} p_{21}^{\mathrm{L'}}(x) = \exp(-\int_0^{\Delta_{21}^{\mathrm{L'}}(x)} \Pr_1^{\mathrm{L}}(u) 2\pi u \lambda_1 du), \\ \Delta_{21}^{\mathrm{L'}}(x) = (\frac{P_1}{P_2})^{\frac{1}{\alpha_1^{\mathrm{L}}}} \times (\frac{A_1^{\mathrm{L}}}{A_2^{\mathrm{L}}})^{\frac{1}{\alpha_1^{\mathrm{L}}}} \times x^{\frac{\alpha_2^{\mathrm{L}}}{\alpha_1^{\mathrm{L}}}}; \\ p_{22}^{\mathrm{L'}}(x) = \exp(-\int_0^{\Delta_{22}^{\mathrm{L'}}(x)} \Pr_1^{\mathrm{NL}}(u) 2\pi u \lambda_1 du), \\ \Delta_{22}^{\mathrm{L'}}(x) = (\frac{P_1}{P_2})^{\frac{1}{\alpha_1^{\mathrm{NL}}}} \times (\frac{A_1^{\mathrm{NL}}}{A_2^{\mathrm{L}}})^{\frac{1}{\alpha_1^{\mathrm{NL}}}} \times x^{\frac{\alpha_2^{\mathrm{L}}}{\alpha_1^{\mathrm{NL}}}}, \end{cases} \tag{60}$$

and

$$\begin{cases} p_{21}^{\mathrm{NL'}}(x) = \exp(-\int_0^{\Delta_{21}^{\mathrm{NL'}}(x)} \Pr_1^{\mathrm{L}}(u) 2\pi u \lambda_1 du), \\ \Delta_{21}^{\mathrm{NL'}}(x) = (\frac{P_1}{P_2})^{\frac{1}{\alpha_1^{\mathrm{L}}}} \times (\frac{A_1^{\mathrm{L}}}{A_2^{\mathrm{NL}}})^{\frac{1}{\alpha_1^{\mathrm{L}}}} \times x^{\frac{\alpha_2^{\mathrm{NL}}}{\alpha_1^{\mathrm{L}}}}; \\ p_{22}^{\mathrm{NL'}}(x) = \exp(-\int_0^{\Delta_{22}^{\mathrm{NL'}}(x)} \Pr_1^{\mathrm{NL}}(u) 2\pi u \lambda_1 du), \\ \Delta_{22}^{\mathrm{NL'}}(x) = (\frac{P_1}{P_2})^{\frac{1}{\alpha_1^{\mathrm{NL}}}} \times (\frac{A_1^{\mathrm{NL}}}{A_2^{\mathrm{NL}}})^{\frac{1}{\alpha_1^{\mathrm{NL}}}} \times x^{\frac{\alpha_2^{\mathrm{NL}}}{\alpha_1^{\mathrm{NL}}}}, \end{cases} \tag{61}$$

respectively.

Then we focus on the derivation of the SINR. Take the case $u \in \mathcal{U}_1^{\mathrm{L}}$ for example, for the typical user u, the coverage probability of the LoS MBS is given as

$$\begin{aligned} \mathcal{S}_1^{\mathrm{L}}(\tau) &= \mathbb{E}_x\left\{\mathbb{P}[\mathrm{SINR}_1^{\mathrm{L}}(x) > \tau]\right\} \\ &= \int_0^\infty \mathbb{P}[\mathrm{SINR}_1^{\mathrm{L}}(x) > \tau] \mathcal{F}_1^{\mathrm{L}}(x) dx. \end{aligned} \tag{62}$$

The UE SINR in (62) is rewritten as $\gamma(x) = \frac{S_1^{\mathrm{L}}(x)h_{1,0}}{I_{agg}+\sigma^2}$, where $S_1^{\mathrm{L}}(x) = P_1 A_1^{\mathrm{L}} x^{-\alpha_1^{\mathrm{L}}}$ and I_{agg} denotes the aggregative interference, which comes from the other active MBSs and SBSs. So the CCDF of the typical user SINR at distance x from its associated LoS MBS is given as

$$\mathbb{P}[\gamma(x) > \tau] = \mathbb{P}\left\{h_{1,0} > \frac{(I_x+\sigma^2)\tau}{S_1^{\mathrm{L}}(x)}\right\} = \exp(\frac{-\sigma^2\tau}{S_1^{\mathrm{L}}(x)})\mathcal{L}_{I_1^{\mathrm{L}}}(\frac{\tau}{S_1^{\mathrm{L}}(x)}), \quad (63)$$

and the Laplace transform of I_x is shown on the top of next page.

The results from other cases that $u \in \{\mathcal{U}_1^{\mathrm{NL}}\}$ can be obtained by the similar approach. For the case that $u \in \{\mathcal{U}_2^{\mathrm{L}}, \mathcal{U}_2^{\mathrm{NL}}\}$, the SINR consitutes 2 parts. The first part follows the same logic with that $u \in \{\mathcal{U}_1\}$ and constitutes a θ proportion of the whole unit, while the second part does not consider the mutual interference from the MBSs.

In the following, we turn to the case that $u \in \mathcal{U}_3$. Following the same approach, we first show how to compute the PDF $F_3^{\mathrm{L}}(x)$ in (19), as shown at the top of the previous page. To this end, we define two events as follow.

- Event Biased-SB$^{\mathrm{L}}$: The nearest biased small BS with a LoS path to the UE is located at distance X^{L} with no other BSs outperforming the associated BS. According to the proof of Lemma 1, the PDF of X^{L} is written as
$$f_X^{\mathrm{L}}(x) = p_{21}^{\mathrm{L}}(x) \times p_{22}^{\mathrm{L}}(x) \times p_{23}^{\mathrm{L}}(x) \times f_2^{\mathrm{L}}(x). \quad (65)$$
- Event MB conditioned on the value of X^{L}: Given that $\mathrm{X}^{\mathrm{L}} = x$, the UE is associated with a biased LoS small BS with distance X^{L}, which is offloaded from a macro BS with a LoS path at distance $\mathrm{y}_1^{\mathrm{L}}$ (Event MB$^{\mathrm{L}}$) or a macro BS with a NLoS path at distance $\mathrm{y}_1^{\mathrm{NL}}$ (Event MB$^{\mathrm{NL}}$).
  - Event MB$^{\mathrm{L}}$ conditioned on the value of X^{L}: To make sure that the UE was associated with the LoS MB with distance $\mathrm{y}_1^{\mathrm{L}}$ before the power biasing process, there should be no other BSs having stronger signal than the associated one. Such conditional probability of MB$^{\mathrm{L}}$ on condition of $\mathrm{X}^{\mathrm{L}} = x$ is
  $$\mathfrak{p}_1^{\mathrm{L}}(x) = \int_0^{y_1^{\mathrm{L}}} p_{11}^{\mathrm{L}}(y_1^{\mathrm{L}}) \times p_{12}^{\mathrm{L}}(y_1^{\mathrm{L}}) \times p_{13}^{\mathrm{L}}(y_1^{\mathrm{L}}) \times f_1^{\mathrm{L}}(y_1^{\mathrm{L}})dx, \quad (66)$$
  where y_1^{L} satisfies $y_1^{\mathrm{L}} = \arg\{S_2^{\mathrm{L}}(y_1^{\mathrm{L}}) \times D = S_1^{\mathrm{L}}(x)\}$.
  - Event MB $^{\mathrm{NL}}$ conditioned on the value of X^{L}: Similar to the event MB$^{\mathrm{L}}$, the conditional probability is
  $$\mathfrak{p}_1^{\mathrm{NL}}(x) = \int_0^{y_1^{\mathrm{NL}}} p_{11}^{\mathrm{NL}}(y_1^{\mathrm{NL}}) \times p_{12}^{\mathrm{NL}}(y_1^{\mathrm{NL}}) \times p_{13}^{\mathrm{NL}}(y_1^{\mathrm{NL}}) \times f_1^{\mathrm{NL}}(y_1^{\mathrm{NL}})dx, \quad (67)$$
  where y_1^{NL} satisfies $y_1^{\mathrm{NL}} = \arg\{S_2^{\mathrm{L}}(y_1^{\mathrm{NL}}) \times D = S_1^{\mathrm{NL}}(x)\}$.

Thus, the expression of $\mathcal{F}_3^{L}(x)$ can be written as

$$\mathcal{F}_3^{\mathrm{L}}(x) = p_{21}^{\mathrm{L}}(x) \times p_{22}^{\mathrm{L}}(x) \times p_{23}^{\mathrm{L}}(x) \times \left(\mathfrak{p}_1^{\mathrm{L}}(x) + \mathfrak{p}_1^{\mathrm{NL}}(x)\right) \times f_2^{\mathrm{L}}(x). \quad (68)$$

Similarly, the expression of $\mathcal{F}_3^{NL}(x)$ is written as

$$\mathcal{F}_3^{\mathrm{NL}}(x) = p_{21}^{\mathrm{NL}}(x) \times p_{22}^{\mathrm{NL}}(x) \times p_{23}^{\mathrm{NL}}(x) \times \left(\mathfrak{p}_2^{\mathrm{L}}(x) + \mathfrak{p}_2^{\mathrm{NL}}(x)\right) \times f_2^{\mathrm{NL}}(x), \quad (69)$$

where $\mathfrak{p}_2^{\mathrm{L}}(x) = \int_0^{y_2^{\mathrm{L}}} p_{11}^{\mathrm{L}}(y_2^{\mathrm{L}}) \times p_{12}^{\mathrm{L}}(y_2^{\mathrm{L}}) \times p_{13}^{\mathrm{L}}(y_2^{\mathrm{L}}) \times f_1^{\mathrm{L}}(y_2^{\mathrm{L}})dx$, and y_2^{L} satisfies $y_2^{\mathrm{L}} = \arg\{S_2^{\mathrm{NL}}(y_2^{\mathrm{L}}) \times D = S_1^{\mathrm{L}}(x)\}$, and $\mathfrak{p}_2^{\mathrm{NL}}(x) = \int_0^{y_2^{\mathrm{NL}}} p_{11}^{\mathrm{NL}}(y_2^{\mathrm{NL}}) \times p_{12}^{\mathrm{NL}}(y_2^{\mathrm{NL}}) \times p_{13}^{\mathrm{NL}}(y_2^{\mathrm{NL}}) \times f_1^{\mathrm{NL}}(y_2^{\mathrm{NL}})dx$, and y_2^{NL} satisfies $y_2^{\mathrm{NL}} = \arg\{S_2^{\mathrm{NL}}(y_2^{\mathrm{NL}}) \times D = S_1^{\mathrm{NL}}(x)\}$.

The calculation of SINR for $u \in \mathcal{U}_3$ is similar with other cases and it only consider the interference from the SBSs, thus the rest proof is omitted. Therefore, the overall SINR coverage of a typical user cab then be obtained using the law of total probability to get $\mathcal{S}(\tau) = \sum_l \mathcal{S}_l(\tau)$.

APPENDIX D
PROOF OF THEOREM 2

From (30), the ASE of the k-th tier is

$$\mathcal{R}_k = \int_0^{\infty} \left\{\mathbb{E}_{\mathrm{SINR}_k}[\log_2(1+\mathrm{SINR}_k(x))]\right\} \mathcal{F}_k(x)dx, \quad (70)$$

where $\mathcal{F}_k(x)$ is given in Theorem 1. Since $\mathbb{E}[R] = \int_0^{\infty} \mathbb{P}[X > x]dx$ for $X > 0$, we can obtain

$$\begin{aligned}&\mathbb{E}_{\mathrm{SINR}_k}[\log_2(1+\mathrm{SINR}_k(x))] \\ &= \int_0^{\infty} \mathbb{P}\left\{\log_2[1+\mathrm{SINR}_k(x)] > \rho\right\} d\rho \\ &= \int_{\log_2(\tau+1)}^{\infty} \mathbb{P}\left(\mathrm{SINR}_k(x) > 2^{\rho}-1\right) d\rho \end{aligned} \quad (71)$$

The rest proof is similar with Appendix A, and the result is obtained from plugging $\tau = 2^{\rho}-1$, conditioned on the $\mathrm{SINR}_k(x) > \tau$.

For the users belong to $\mathcal{U}_2$, because of the resource partitioning, they can be served in all time-slots. Thus, the calculation of their ergodic rate is composed of two parts. When the macro BS schedule ABSs, the users in $\mathcal{U}_2$ would not get interference from tier 1 BSs and they share the η fraction of channel resource with range expanded UEs, whereas the mutual interference would be considered when the macro BSs are working, in which $1-\eta$ fraction of resource is allocated to the users in $\mathcal{U}_1$ and $\mathcal{U}_2$.

APPENDIX E
PROOF OF LEMMA 9

As $\lambda_2 \to +\infty$, all the UEs are assumed to be connect to BSs with LoS channel, so the path loss $\zeta(r)$ can be rewritten as

$$\zeta_k(r) = \zeta_k^{\mathrm{L}}(r) = A_k^{\mathrm{L}} r^{-\alpha_k^{\mathrm{L}}}, \mathrm{LoS}: \Pr_k^{\mathrm{L}}(r) = 1. \quad (72)$$

Thus, the components for the NLoS part in R, which are $\mathcal{R}_1^{NL}$, $\mathcal{R}_2^{NL}$ and $\mathcal{R}_3^{NL}$, can be neglected. Furthermore, the interference power $\mathcal{L}_{I_1^L}(\frac{t(\rho)}{S_1^L(x)})$ can be written as

$$\mathcal{L}_{I_1^L}(s) = \exp\left(-2\pi\tilde{\lambda}_1\left(\int_x^{\infty} 1 \times \frac{u}{1+\frac{S_1^L(x)}{\tau S_1^L(u)}}du\right)\right)$$

The Laplace transform of I_x is shown as follows:

$$\begin{aligned}\mathcal{L}_{I_1^{\mathrm{L}}}\left(\frac{\tau}{S_1^{\mathrm{L}}(x)}\right) &\overset{(a)}{=} \exp\left\{-2\pi\tilde{\lambda}_1\int_x^{\infty}\Pr_1^{\mathrm{L}}(u)\left[1-E_{[g]}\left(\exp\left(-\frac{g\tau S_1^{\mathrm{L}}(u)}{S_1^{\mathrm{L}}(x)}\right)\right)\right]udu\right\}\\ &\times\exp\left\{-2\pi\tilde{\lambda}_1\int_{\Delta_{11}^{\mathrm{L}}(x)}^{\infty}\left(1-\Pr_1^{\mathrm{L}}(u)\right)\left[1-E_{[g]}\left(\exp\left(-\frac{g\tau S_1^{\mathrm{NL}}(u)}{S_1^{\mathrm{L}}(x)}\right)\right)\right]udu\right\}\\ &\times\exp\left\{-2\pi\tilde{\lambda}_2\int_{\Delta_{12}^{\mathrm{L}'}(x)}^{\infty}\Pr_2^{\mathrm{L}}(u)\left[1-E_{[g]}\left(\exp\left(-\frac{g\tau S_2^{\mathrm{L}}(u)}{S_1^{\mathrm{L}}(x)}\right)\right)\right]udu\right\}\\ &\times\exp\left\{-2\pi\tilde{\lambda}_2\int_{\Delta_{13}^{\mathrm{L}'}(x)}^{\infty}\left(1-\Pr_2^{\mathrm{L}}(u)\right)\left[1-E_{[g]}\left(\exp\left(-\frac{g\tau S_2^{\mathrm{NL}}(u)}{S_1^{\mathrm{L}}(x)}\right)\right)\right]udu\right\}\\ &=\exp\left(-2\pi\tilde{\lambda}_1\left(\int_x^{\infty}\Pr_1^{L}(u)\frac{u}{1+\frac{S_1^{L}(x)}{\tau S_1^{L}(u)}}du+\int_{\Delta_{11}^{L}(x)}^{\infty}\Pr_1^{NL}(u)\frac{u}{1+\frac{S_1^{L}(x)}{\tau S_1^{NL}(u)}}du\right)\right)\\ &\times\exp\left(-2\pi\tilde{\lambda}_2\left(\int_{\Delta_{12}^{L}(x)}^{\infty}\Pr_2^{L}(u)\frac{u}{1+\frac{S_1^{L}(x)}{\tau S_2^{L}(u)}}du+\int_{\Delta_{13}^{L}(x)}^{\infty}\Pr_2^{NL}(u)\frac{u}{1+\frac{S_1^{L}(x)}{\tau S_2^{NL}(u)}}du\right)\right),\end{aligned}\tag{64}$$

where step (a) states that the closest interferer from each type of BSs.

$$\begin{aligned}&\times\exp\left(-2\pi\tilde{\lambda}_2\left(\int_{\Delta_{12}^{L}(x)}^{\infty}1\times\frac{u}{1+\frac{S_1^{L}(x)}{\tau S_2^{L}(u)}}du\right)\right)\\ &=\exp\left(-2\pi\tilde{\lambda}_1\left(\int_x^{\infty}1\times\frac{u}{1+\left(\tau^{-1}x^{-\alpha_1^{L}}\right)u^{\alpha_1^{L}}}du\right)\right)\\ &\times\exp\left(-2\pi\tilde{\lambda}_2\left(\int_x^{\infty}1\times\frac{u}{1+\left(\frac{P_1A_1^{L}}{P_2A_2^{L}\tau x^{\alpha_1^{L}}}\right)u^{\alpha_2^{L}}}du\right)\right).\end{aligned}\tag{73}$$

In order to evaluate (73), we define the following integral functions according to [27],

$$\begin{aligned}&\rho(\alpha,\beta,t,d)\\ &=\int_d^{\infty}\frac{u^{\beta}}{1+tu^{\alpha}}du\\ &=\left[\frac{d^{-(\alpha-\beta-1)}}{t(\alpha-\beta-1)}\right]F_1\left[1,1-\frac{\beta+1}{\alpha};2-\frac{\beta+1}{\alpha};-\frac{1}{td^{\alpha}}\right],\\ &\qquad(\alpha>\beta+1),\end{aligned}\tag{74}$$

where ${}_2F_1[\cdot,\cdot;\cdot;\cdot]$ is the hyper-geometric function [27]. Our proof is completed by plugging (74) into (73), and the calculations of $\mathcal{L}_{I_{21}^{L}}(\frac{t(\rho)}{S_2^{L}(x)})$, $\mathcal{L}_{I_{22}^{L}}(\frac{t(\rho)}{S_2^{L}(x)})$, and $\mathcal{L}_{I_3^{L}}(\frac{t(\rho)}{S_2^{L}(x)})$ are following similar procedure, and is omitted here.

REFERENCES

[1] *Visual Networking Index Forecast, 2015–2020*, Cisco, San Jose, CA, USA, 2015.

[2] D. López-Pérez, M. Ding, H. Claussen, and A. H. Jafari, "Towards 1 Gbps/UE in cellular systems: Understanding ultra-dense small cell deployments," *IEEE Commun. Surveys Tuts.*, vol. 17, no. 4, pp. 2078–2101, 4th Quart. 2015.

[3] B. Zhuang, D. Guo, and M. L. Honig, "Energy-efficient cell activation, user association, and spectrum allocation in heterogeneous networks," *IEEE J. Sel. Areas Commun.*, vol. 34, no. 4, pp. 823–831, Apr. 2016.

[4] Q. Ye, B. Rong, Y. Chen, M. Al-Shalash, C. Caramanis, and J. G. Andrews, "User association for load balancing in heterogeneous cellular networks," *IEEE Trans. Wireless Commun.*, vol. 12, no. 6, pp. 2706–2716, Jun. 2013.

[5] M. Di Renzo, "Stochastic geometry modeling and analysis of multi-tier millimeter wave cellular networks," *IEEE Trans. Wireless Commun.*, vol. 14, no. 9, pp. 5038–5057, Sep. 2015.

[6] M. Di Renzo, A. Guidotti, and G. E. Corazza, "Average rate of downlink heterogeneous cellular networks over generalized fading channels: A stochastic geometry approach," *IEEE Trans. Commun.*, vol. 61, no. 7, pp. 3050–3071, Jul. 2013.

[7] J. G. Andrews, F. Baccelli, and R. K. Ganti, "A tractable approach to coverage and rate in cellular networks," *IEEE Trans. Commun.*, vol. 59, no. 11, pp. 3122–3134, Nov. 2011.

[8] H. S. Dhillon, R. K. Ganti, F. Baccelli, and J. G. Andrews, "Modeling and analysis of K-tier downlink heterogeneous cellular networks," *IEEE J. Sel. Areas Commun.*, vol. 30, no. 3, pp. 550–560, Apr. 2012.

[9] X. Zhang and J. G. Andrews, "Downlink cellular network analysis with multi-slope path loss models," *IEEE Trans. Commun.*, vol. 63, no. 5, pp. 1881–1894, May 2015.

[10] M. Ding, P. Wang, D. López-Pérez, G. Mao, and Z. Lin, "Performance impact of LOS and NLoS transmissions in dense cellular networks," *IEEE Trans. Wireless Commun.*, vol. 15, no. 3, pp. 2365–2380, Mar. 2016.

[11] A. AlAmmouri, J. G. Andrews, and F. Baccelli. (2017). "SINR and throughput of dense cellular networks with stretched exponential path loss." [Online]. Available: https://arxiv.org/abs/1703.08246

[12] S. Lee and K. Huang, "Coverage and economy of cellular networks with many base stations," *IEEE Commun. Lett.*, vol. 16, no. 7, pp. 1038–1040, Jul. 2012.

[13] M. Di Renzo, W. Lu, and P. Guan, "The intensity matching approach: A tractable stochastic geometry approximation to system-level analysis of cellular networks," *IEEE Trans. Wireless Commun.*, vol. 15, no. 9, pp. 5963–5983, Sep. 2016.

[14] S. M. Yu and S.-L. Kim, "Downlink capacity and base station density in cellular networks," in *Proc. 11th Int. Symp. Modeling Optim. Mobile, Ad Hoc Wireless Netw. (WiOpt)*, 2013, pp. 119–124.

[15] M. Ding, D. L. Perez, G. Mao, and Z. Lin. (2016). "Study on the idle mode capability with LoS and NLoS transmissions." [Online]. Available: https://arxiv.org/abs/1608.06694

[16] H.-S. Jo, Y. J. Sang, P. Xia, and J. G. Andrews, "Outage probability for heterogeneous cellular networks with biased cell association," in *Proc. IEEE Global Telecommun. Conf. (GLOBECOM)*, Dec. 2011, pp. 1–5.

[17] A. Damnjanovic *et al.*, "A survey on 3GPP heterogeneous networks," *IEEE Wireless Commun.*, vol. 18, no. 3, pp. 10–21, Jun. 2011.

[18] D. López-Pérez, I. Guvenc, G. De la Roche, M. Kountouris, T. Q. S. Quek, and J. Zhang, "Enhanced intercell interference coordination challenges in heterogeneous networks," *IEEE Wireless Commun.*, vol. 18, no. 3, pp. 22–30, Jun. 2011.

[19] M. Ding and D. López-Pérez. (2017). "On the performance of practical ultra-dense networks: The major and minor factors." [Online]. Available: https://arxiv.org/abs/1701.07964
[20] Y. Li, B. Cao, and C. Wang, "Handover schemes in heterogeneous LTE networks: Challenges and opportunities," *IEEE Wireless Commun.*, vol. 23, no. 2, pp. 112–117, Apr. 2016.
[21] R. Balakrishnan and I. Akyildiz, "Local anchor schemes for seamless and low-cost handover in coordinated small cells," *IEEE Trans. Mobile Comput.*, vol. 15, no. 5, pp. 1182–1196, May 2016.
[22] H.-S. Jo, Y. J. Sang, P. Xia, and J. G. Andrews, "Heterogeneous cellular networks with flexible cell association: A comprehensive downlink SINR analysis," *IEEE Trans. Wireless Commun.*, vol. 11, no. 10, pp. 3484–3495, Oct. 2012.
[23] C. Ma, M. Ding, H. Chen, Z. Lin, G. Mao, and D. López-Pérez. (2017). "On the performance of multi-tier heterogeneous cellular networks with idle mode capability." [Online]. Available: https://arxiv.org/abs/1704.02176
[24] J.-S. Ferenc and Z. Néda, "On the size-distribution of Poisson Voronoi cells," *Phys. A, Statist. Mech. Appl.*, vol. 385, no. 2, pp. 518–526, 2007.
[25] A. L. Hinde and R. E. Miles, "Monte Carlo estimates of the distributions of the random polygons of the Voronoi tessellation with respect to a Poisson process," *J. Statist. Comput. Simul.*, vol. 10, nos. 3–4, pp. 205–223, 1980.
[26] S. Singh, H. S. Dhillon, and J. G. Andrews, "Offloading in heterogeneous networks: Modeling, analysis, and design insights," *IEEE Trans. Wireless Commun.*, vol. 12, no. 5, pp. 2484–2497, May 2013.
[27] I. S. Gradshteyn and I. M. Ryzhik, *Table of Integrals, Series, and Products*. New York, NY, USA: Academic, 2014.
[28] *Further Enhancements to LTE Time Division Duplex (TDD) for Downlink-Uplink (DL-UL) Interference Management and Traffic Adaptation*, document TR 36.828, 3GPP, Jun. 2012.
[29] J. Liu, M. Sheng, L. Liu, and J. Li, "Effect of densification on cellular network performance with bounded pathloss model," *IEEE Commun. Lett.*, vol. 21, no. 2, pp. 346–349, Feb. 2017.
[30] M. Ding, D. López-Pérez, G. Mao, and Z. Lin. (2017). "Ultra-dense networks: Is there a limit to spatial spectrum reuse?" [Online]. Available: https://arxiv.org/abs/1704.00399

Chuan Ma received the B.S. degree from the Beijing University of Posts and Telecommunications, Beijing, China, in 2013. He is currently pursuing the Ph.D. degree in telecommunication from The University of Sydney. His research interests with Dr. Ding and Dr. Lin include stochastic geometry, device-to-device communication, wireless caching networks, and machine learning.

Ming Ding (M'12–SM'17) received the B.S. and M.S. degrees (Hons.) in electronics engineering and the Ph.D. degree in signal and information processing from Shanghai Jiao Tong University, Shanghai, China, in 2004, 2007, and 2011, respectively. From 2007 to 2014, he was with Sharp Laboratories of China, Shanghai, China, as a Researcher/Senior Researcher/Principal Researcher. He also served as the Algorithm Design Director and the Programming Director for a system- level simulator of future telecommunication networks with Sharp Laboratories of China for over seven years. He is currently a Senior Research Scientist with Data61, CSIRO, Sydney, NSW, Australia. He has authored over 50 papers in the IEEE journals and conferences, all in recognized venues, and about 20 3GPP standardization contributions, and a book *Multi-point Cooperative Communication Systems: Theory and Applications* (Springer). Also, as the first inventor, he holds 15 CN, seven JP, three U.S., two KR patents and co-authored over 100 patent applications on 4G/5G technologies. For his inventions and publications, he was a recipient of the President's Award of Sharp Laboratories of China in 2012, and served as one of the key members in the 4G/5G standardization team when it was awarded in 2014 as Sharp Company Best Team: LTE 2014 Standardization Patent Portfolio. He is or has been the Guest Editor/Co-Chair/Co-Tutor/TPC member of several IEEE top-tier journals/conferences, e.g., the IEEE JOURNAL ON SELECTED AREAS IN COMMUNICATIONS, the IEEE *Communications Magazine*, and the IEEE GLOBECOM Workshops.

David López-Pérez (M'12–SM'17) received the B.Sc. and M.Sc. degrees in telecommunication from Miguel Hernandez University, Spain, in 2003 and 2006, respectively, and the Ph.D. degree in wireless networking from the University of Bedfordshire, U.K., in 2011. He is currently a member of Technical Staff with Nokia Bell Labs. He was also a RF Engineer with Vodafone, Spain, from 2005 to 2006, and a Research Associate with King's College London, U.K., from 2010 to 2011. He has authored the book *Small Cell Networks* (IEEE/Wiley Press, 2017), and over 100 book chapters, journal, and conference papers, all in recognized venues. He also holds over 41 patents applications. He was a recipient of the Ph.D. Marie-Curie Fellowship in 2007 and the IEEE ComSoc Best Young Professional Industry Award in 2016. He was also a finalist for the Scientist of the Year prize in The Irish Laboratory Awards in 2013 and 2015. He has been an Editor of the IEEE TRANSACTION ON WIRELESS COMMUNICATIONS since 2016, and he was awarded an Exemplary Reviewer of the IEEE COMMUNICATIONS LETTERS in 2011. He is or has also been a Guest Editor of a number of journals, e.g., the IEEE JOURNAL ON SELECTED AREAS IN COMMUNICATIONS, the IEEE COMMUNICATION MAGAZINE, and the IEEE *Wireless Communication Magazine*.

Zihuai Lin (S'98–M'06–SM'10) received the Ph.D. degree in electrical engineering from the Chalmers University of Technology, Sweden, in 2006. Prior to this he has held positions at Ericsson Research, Stockholm, Sweden. Following Ph.D. graduation, he was a Research Associate Professor with Aalborg University, Denmark. He is currently with the School of Electrical and Information Engineering, The University of Sydney, Australia. His research interests include source/channel/network coding, coded modulation, MIMO, OFDMA, SC-FDMA, radio resource management, cooperative communications, small-cell networks, 5G cellular systems, and IoT.

Jun Li (M'09–SM'16) received the Ph.D. degree in electronic engineering from Shanghai Jiao Tong University, Shanghai, China, in 2009. In 2009, he was with the Department of Research and Innovation, Alcatel Lucent Shanghai Bell, as a Research Scientist. From 2009 to 2012, he was a Post-Doctoral Fellow with the School of Electrical Engineering and Telecommunications, the University of New South Wales, Australia. From 2012 to 2015, he was a Research Fellow with the School of Electrical Engineering, The University of Sydney, Australia. Since 2015, he has been a Professor with the School of Electronic and Optical Engineering, Nanjing University of Science and Technology, Nanjing, China. His research interests include network information theory, channel coding theory, wireless network coding, and cooperative communications. He served as the Technical Program Committee member for several international conferences such as GLOBECOM2015, ICC2014, VTC2014, and ICC2014.

Guoqiang Mao (S'98–M'02–SM'08–F'18) joined the University of Technology Sydney in 2014 as a Professor of wireless networking and the Director of the Center for Real-time Information Networks. Before that, he was with the School of Electrical and Information Engineering, The University of Sydney. He has authored about 200 papers in international conferences and journals, which have been cited over 5000 times. He has been an Editor of the IEEE TRANSACTIONS ON WIRELESS COMMUNICATIONS since 2014 and the IEEE TRANSACTIONS ON VEHICULAR TECHNOLOGY since 2010. His research interest includes intelligent transport systems, applied graph theory and its applications in telecommunications, Internet of Things, wireless sensor networks, wireless localization techniques, and network performance analysis. He is a fellow of IET. He was a recipient of the Top Editor award for outstanding contributions to the IEEE TRANSACTIONS ON VEHICULAR TECHNOLOGY, in 2011, 2014, and 2015, respectively. He is a Co-Chair of IEEE Intelligent Transport Systems Society Technical Committee on Communication Networks. He has served as a Chair, Co-Chair, and TPC member in a large number of international conferences.